A Phenomenological Model Describing the Timing Characteristics of the PICOSEC-Micromegas Detector and Comparison with Detailed Simulations using Garfield++

Konstantinos Paraschou

HEP 2018
Recent Developments in High Energy Physics and Cosmology

This work is part of my master thesis, which I finished recently, under the supervision of Prof. Spyros Tzamarias.

Aristotle University of Thessaloniki

Papers and Support Notes

1) PICOSEC: Charged particle timing at sub-25 picosecond precision with a Micromegas based detector, PICOSEC-RD51 Collaboration, to appear in Nucl. Instrum. Meth. A

2) Single photo-electron timing characteristics of a PICOSEC-Micromegas detector, PICOSEC-RD51 Collaboration, to be published in Nucl. Instrum. Meth. A

3) Evaluation of PICOSEC-Micromegas detectors in muon test beams, PICOSEC-RD51 Collaboration, to be published in Nucl. Instrum. Meth. A

4) Signal production dynamics of the PICOSEC-Micromegas detector, PICOSEC-RD51 Collaboration, under preparation

5) Analysis Methods and Results of the Picosecond-Micromegas Laser Beam Data: PART A – Charge and Amplitude Properties of the PICOSEC Waveforms, AUTH-PICOSEC Team (2017), RD51-NOTE-2017-009. https://espace.cern.ch/test-RD51/RD51%20internal%20notes/RD51-NOTE-2017-009.pdf

6) Analysis Methods and Results of the Picosecond-Micromegas Laser Beam Data: PART B – Timing Characteristics of the PICOSEC Waveforms, AUTH-PICOSEC Team (2017), RD51-NOTE-2017-010. https://espace.cern.ch/test-RD51/RD51%20internal%20notes/RD51-NOTE-2017-010.pdf

7) Analysis Methods and Results of the Picosecond-Micromegas Laser Beam Data: PART C – Simulation of the PICOSEC-Micromegas and Results, AUTH-PICOSEC Team (2017), RD51-NOTE-2017-011. https://espace.cern.ch/test-RD51/RD51%20internal%20notes/RD51-NOTE-2017-011.pdf

The PICOSEC-Micromegas

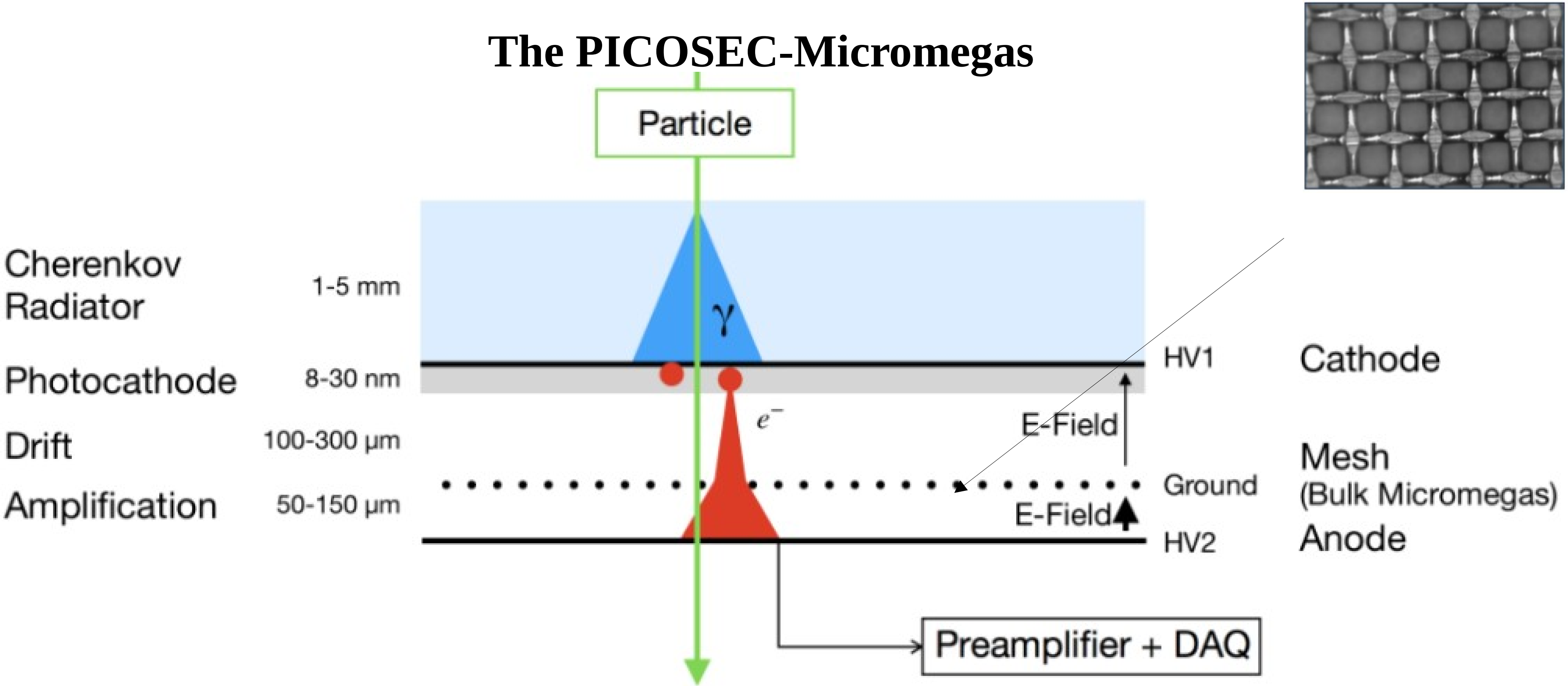

We equip a standard Micromegas with a very thin drift gap and a standard photocathode and use it as a photodetector to detector Cherenkov photons.

The signal induced from both electrons' and ions' motion is detected.

Varying parameters in this study are

Drift Voltage: Voltage Difference between photocathode and mesh

Anode Voltage: Voltage difference between anode and mesh

Laser Test

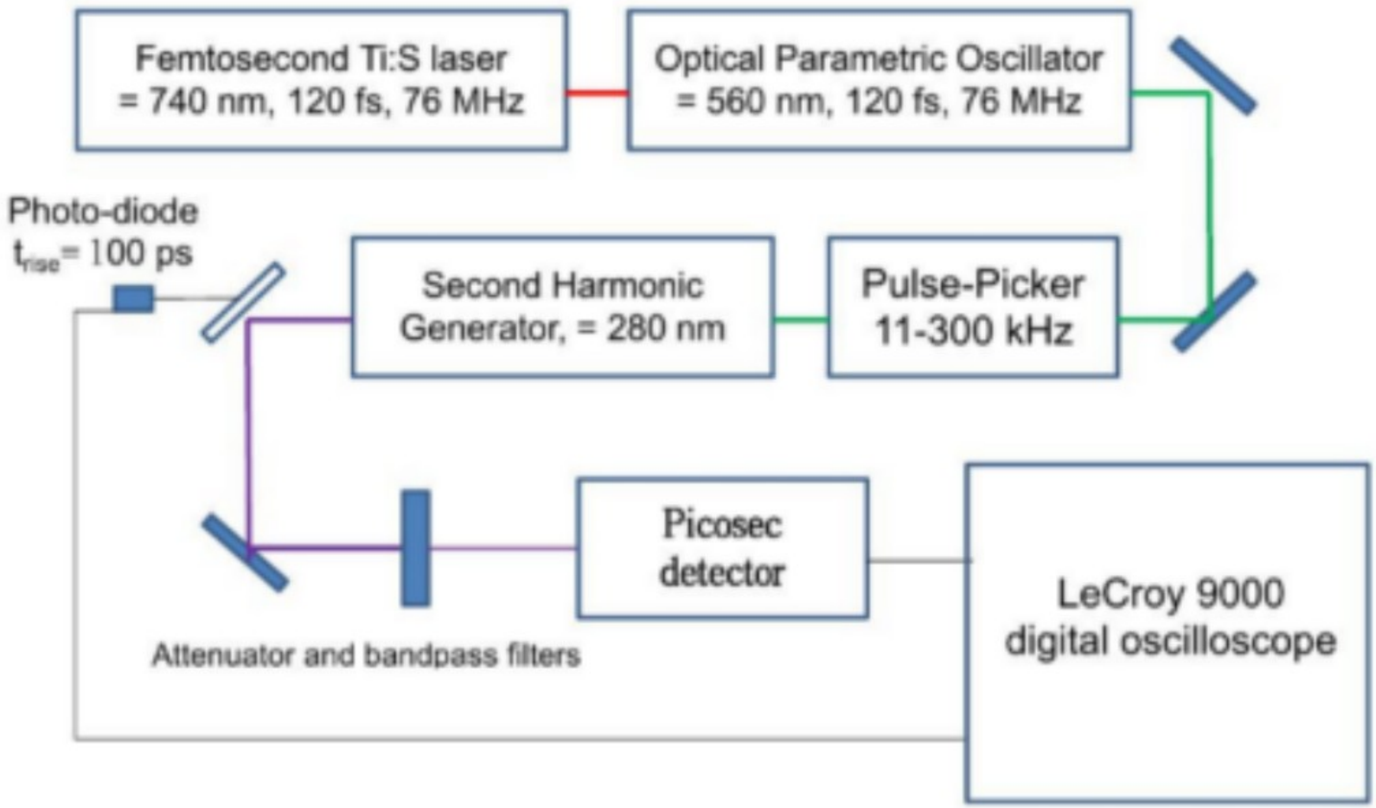

To study a single photoelectron response, we use a fast laser in the IRAMIS facility of CEA-SACLAY. We split the beam to a very fast photodiode and the PICOSEC and then readout the signals with an oscilloscope.

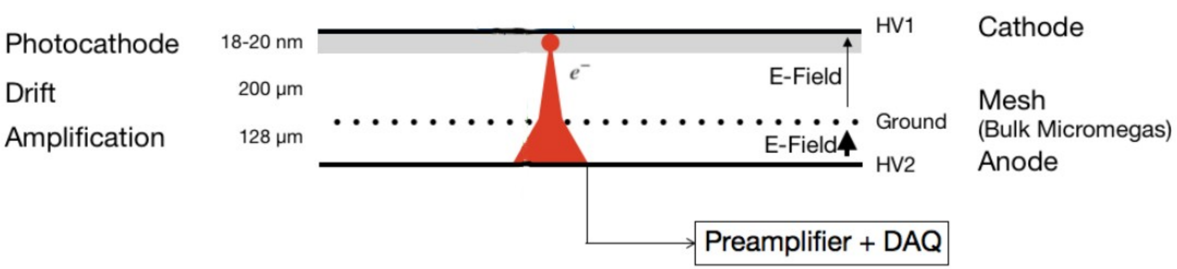

Gas fillings:

1)COMPASS: (1 bar)
80% Ne + 10% CF4 + 10% C2H6

2) CF4: (0.5 bar)
80% CF4 + 20% C2H6

The signal of PICOSEC

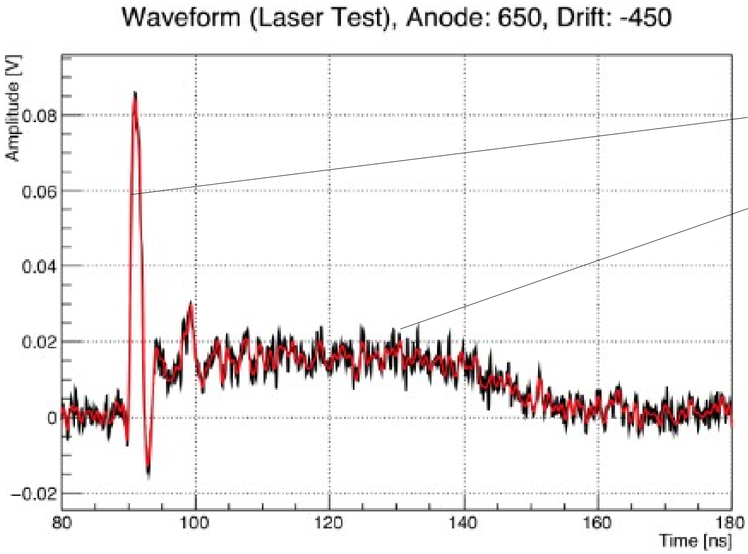

Electron's motion (fast): Electron peak

Ion's motion (slow): Ion tail

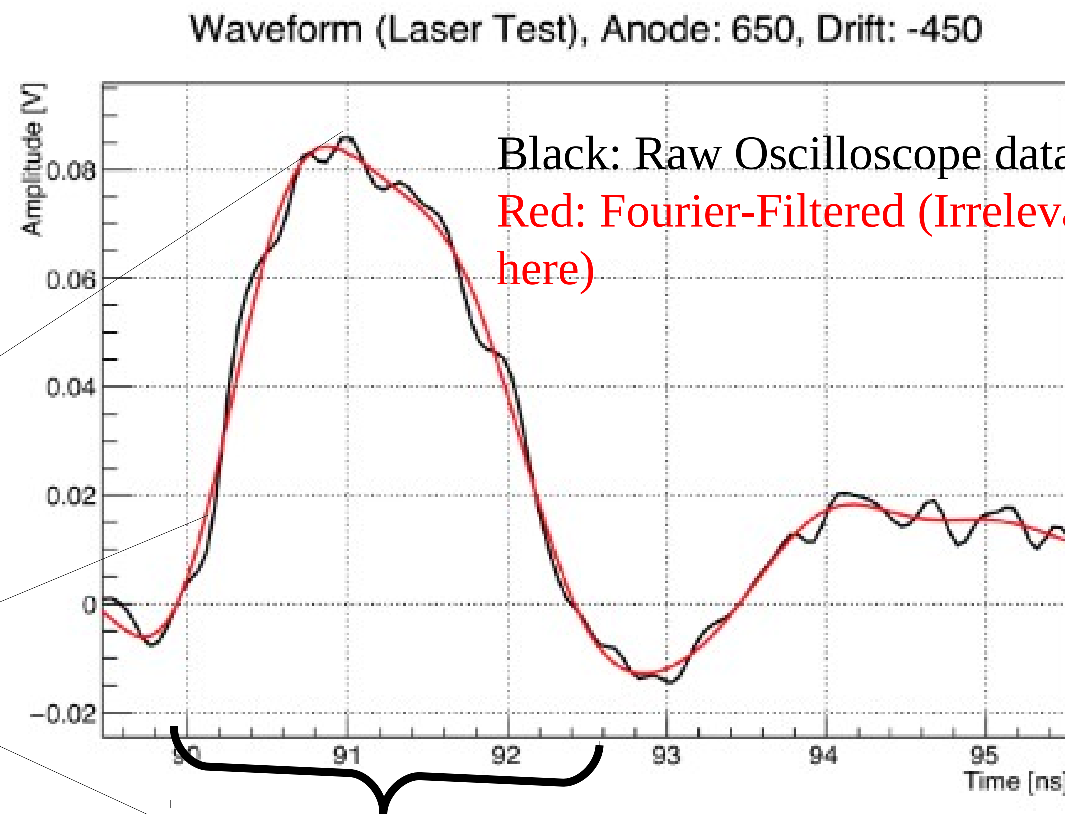

Electron peak amplitude

Electron peak charge

Timing (20% software CFD)

Integral

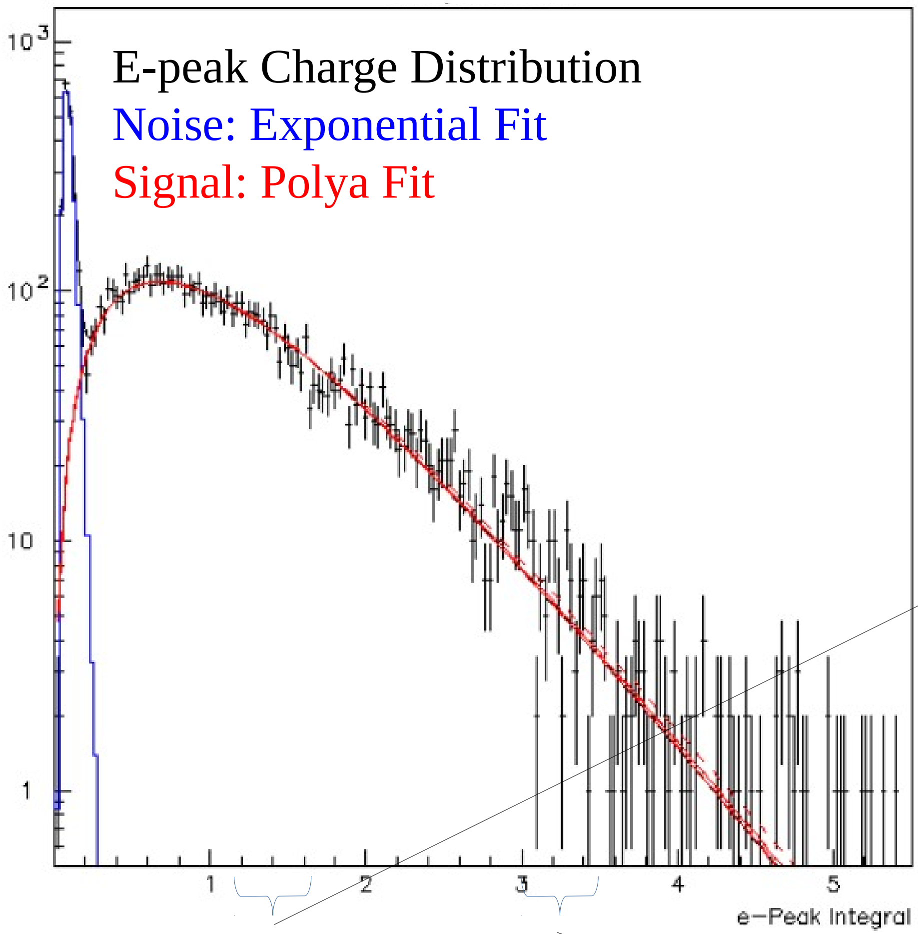

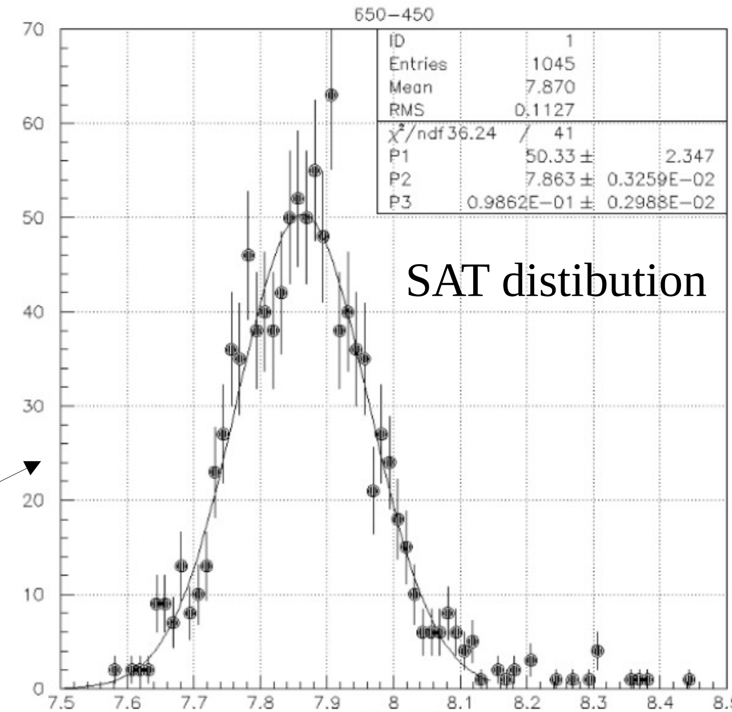

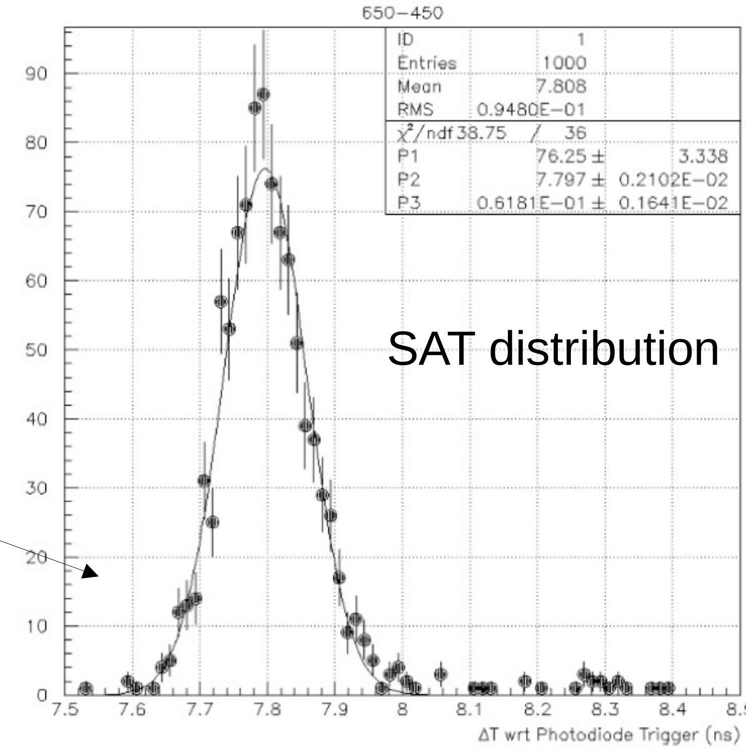

Mean and standard deviation of Signal Arrival Time (SAT) are different for different electron peak charge.

Repeat for all charges and for all different drift voltage settings with a fixed anode voltage (450 V).

(Experimental Data)

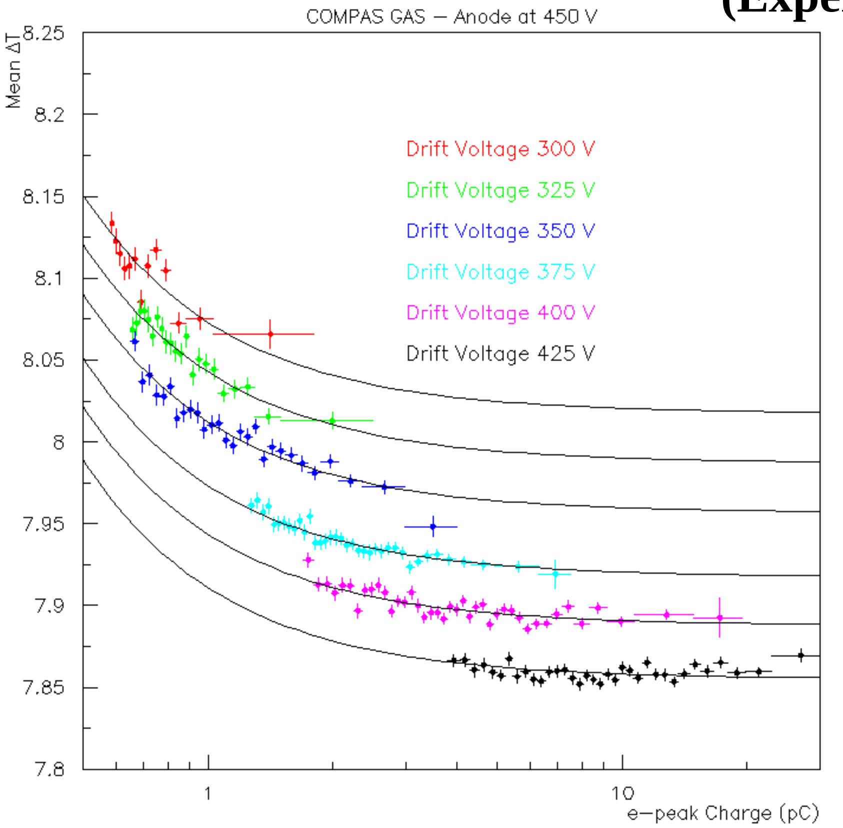

Fig: Mean Signal Arrival Time versus electron peak charge for different Drift Voltage.

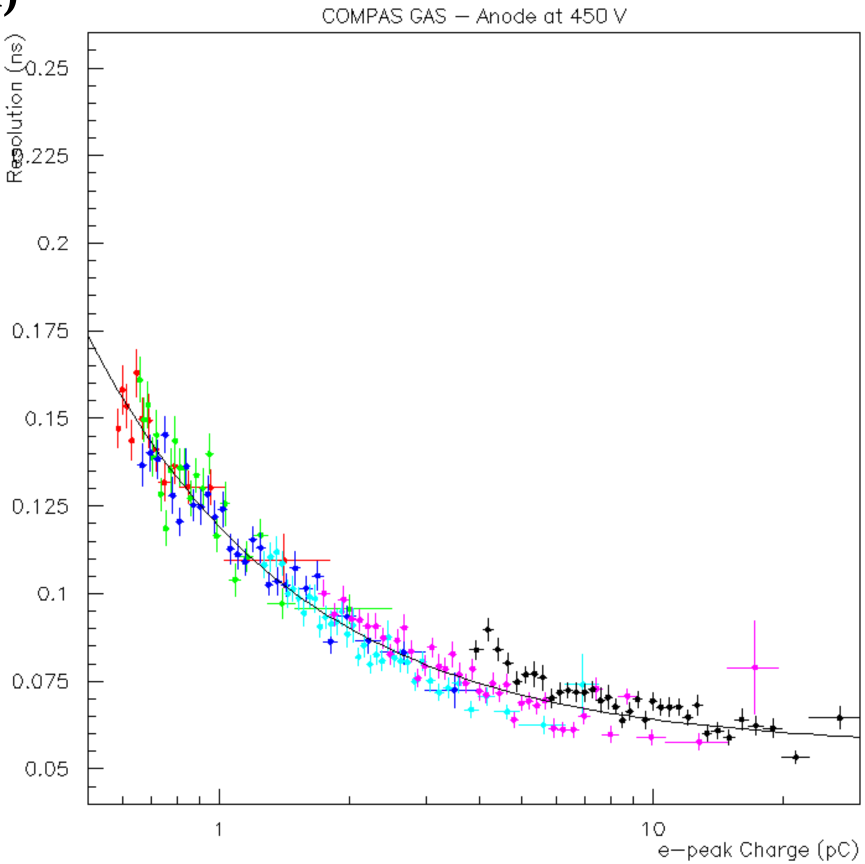

Fig: Time resolution versus electron peak charge for different Drift Voltage.

Parameterize with $f(x) = \frac{b}{x^w} + a$

1.) Large signals arrive faster than smaller ones.

2.) The shape of SAT versus the electron peak charge does not change with the Drift Voltage.

3.) Time resolution versus the electron peak charge does not change with the Drift Voltage.

(Experimental Data)

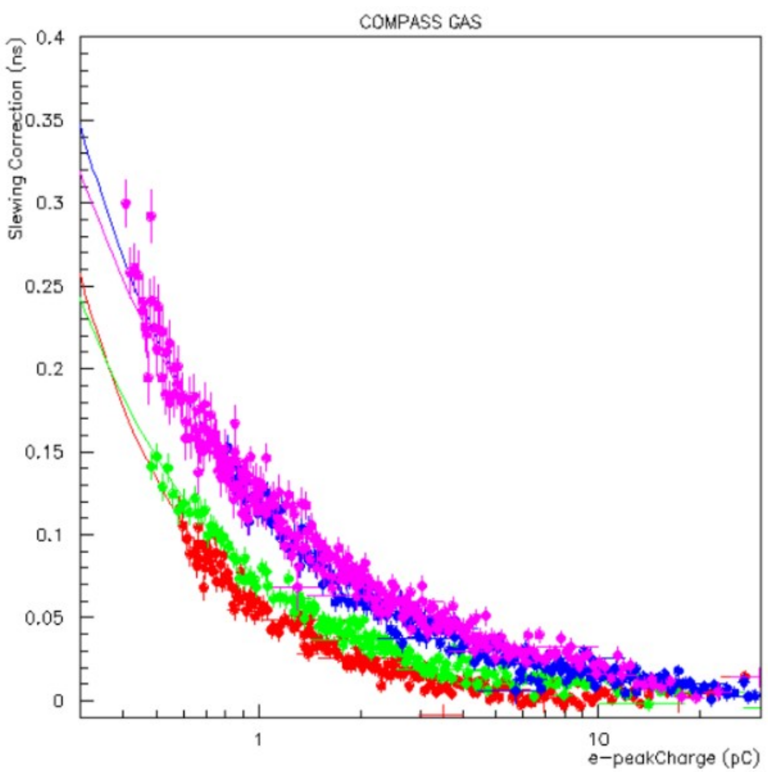

Fig: Mean Signal Arrival Time versus electron peak charge for different Drift Voltage (constant term subtracted).

Anode Voltage:
450 V
475 V
500 V
525 V

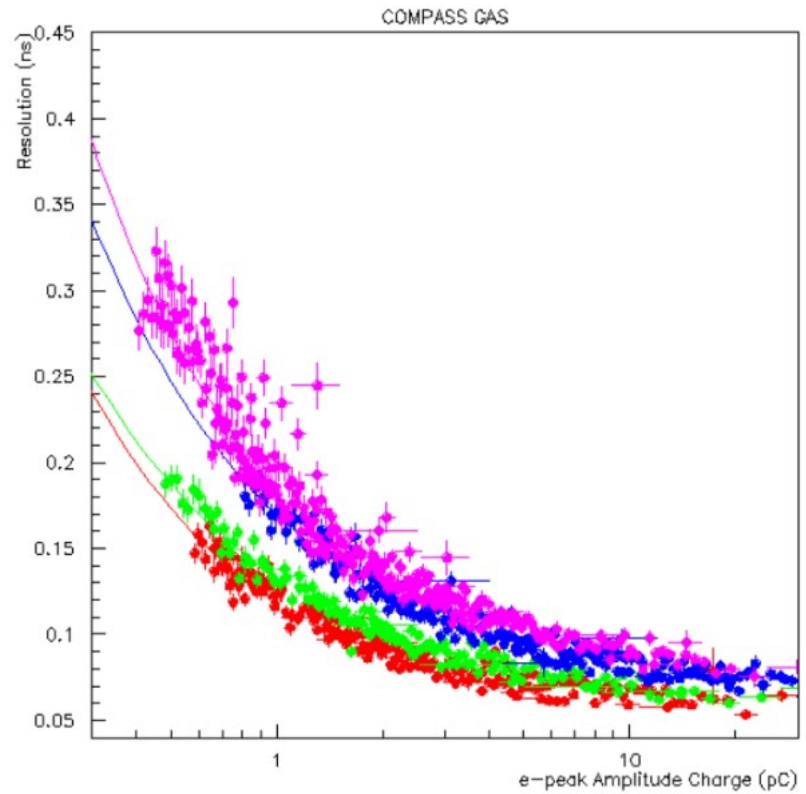

Fig: Time resolution versus electron peak charge for different Drift Voltage.

COMPASS gas

The time resolution gets better by reducing the anode voltage!
This happens because by reducing the anode voltage, the drift voltage must be increased to have the same signal magnitude.

(Experimental Data)

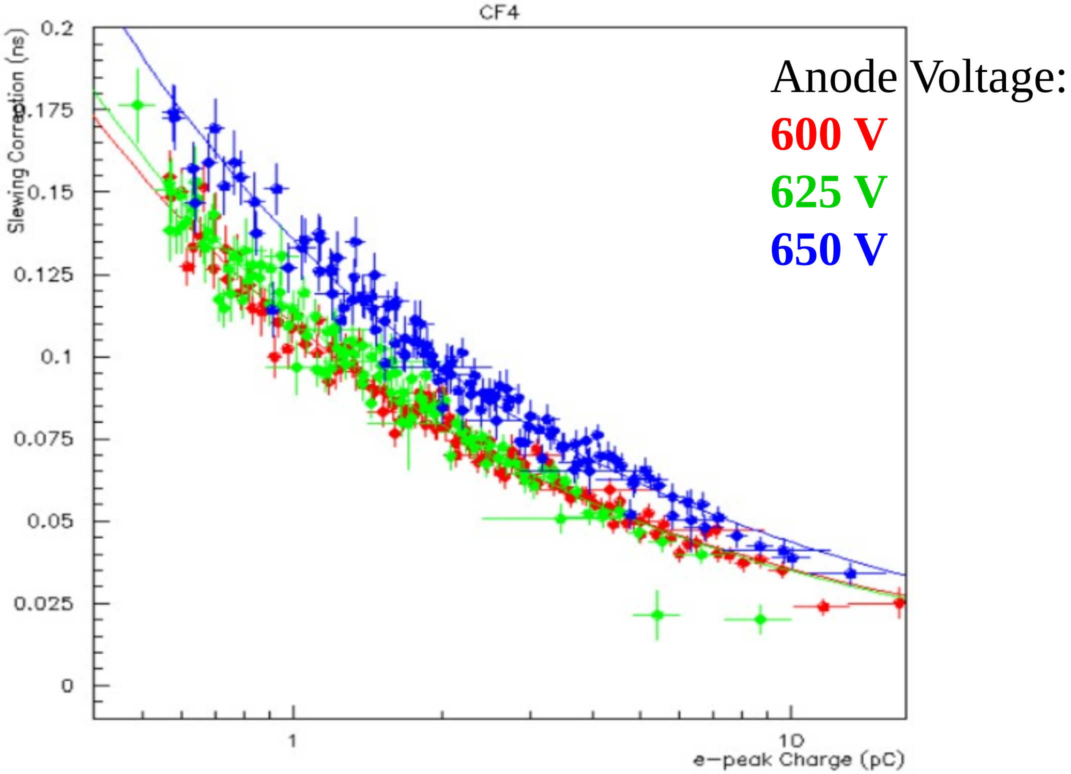

Fig: Mean Signal Arrival Time versus electron peak charge for different Drift Voltage (constant term subtracted).

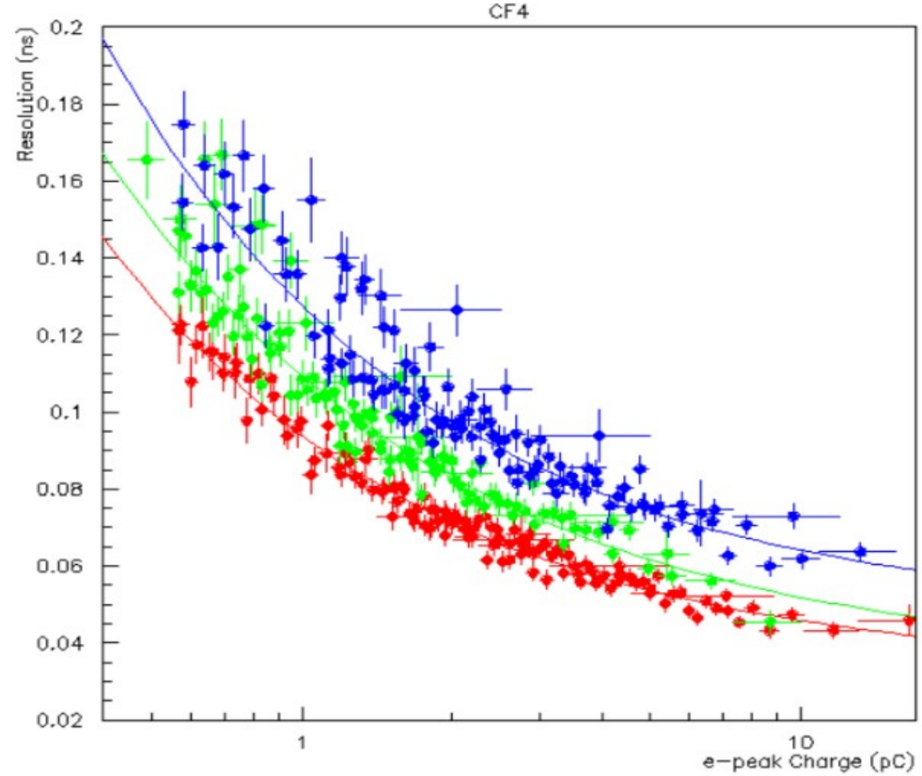

Fig: Time resolution versus electron peak charge for different Drift Voltage.

Same for CF4 gas

The time resolution gets better by reducing the anode voltage!
This happens because by reducing the anode voltage, the drift voltage must be increased to have the same signal magnitude.

Total Time resolution

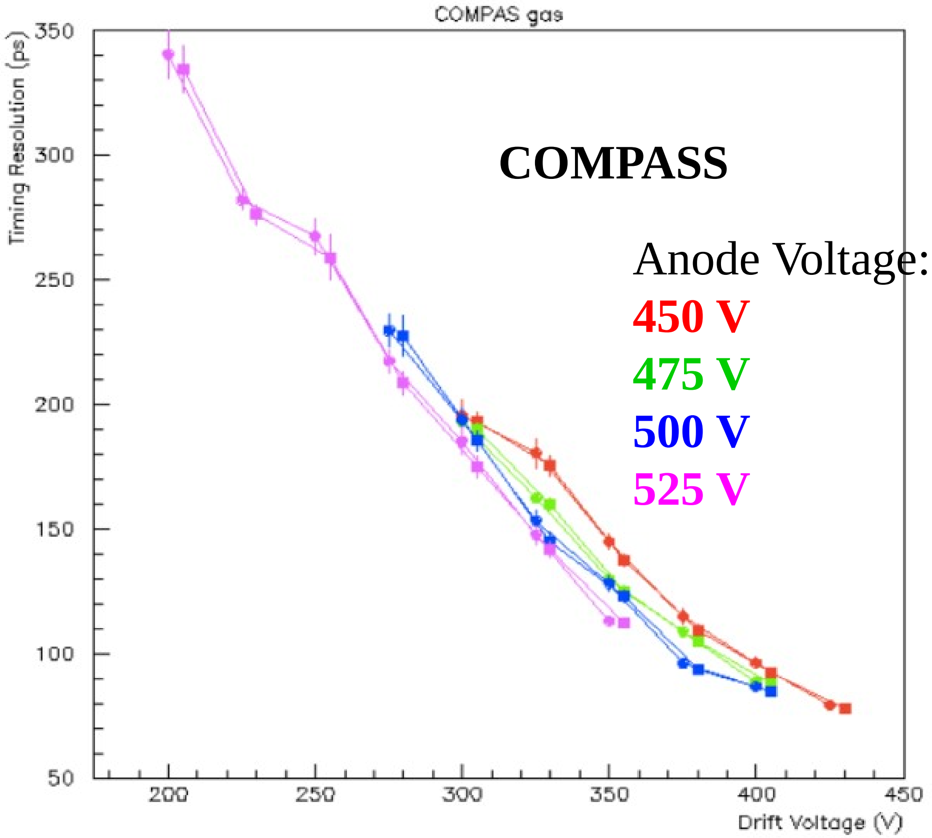

Fig: Total time resolution versus Drift Voltage.

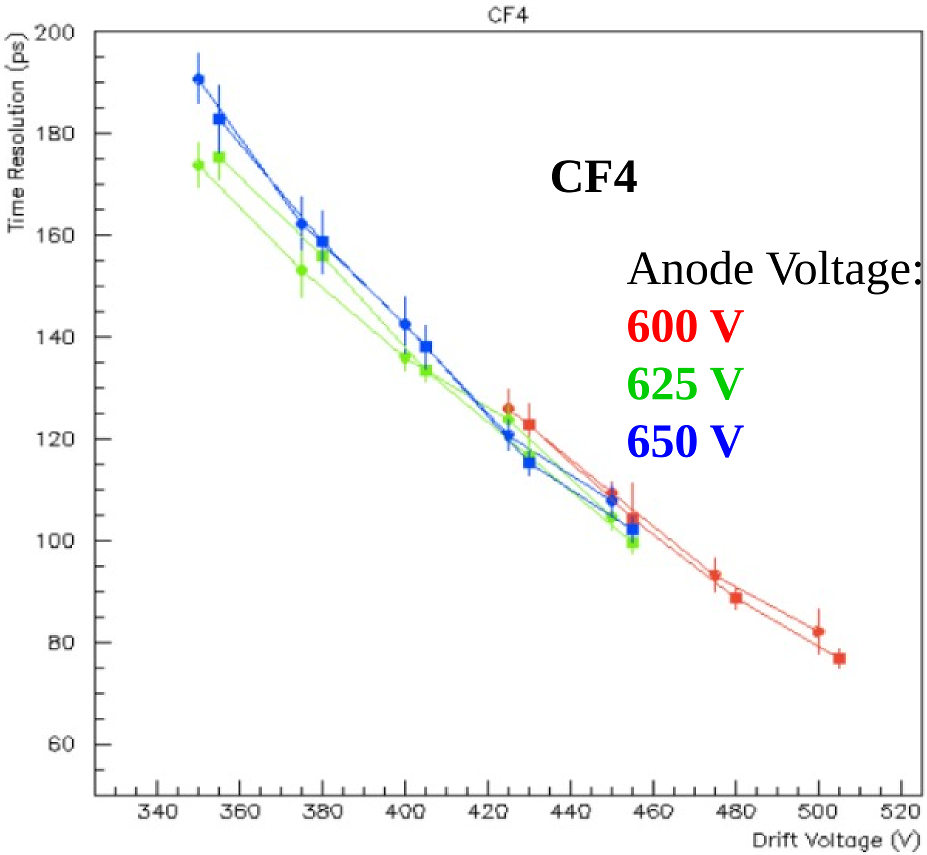

Fig: Total time resolution versus Drift Voltage.

The anode voltage does not affect the total time resolution.

With both gas mixtures we achieve total time resolution < 80 ps.

Optimal time resolution = 76.8 +- 2.0 ps for a SINGLE photoelectron.

Garfield++ Simulation

We use Garfield++ to microscopically simulate the response of the PICOSEC to single photoelectrons.

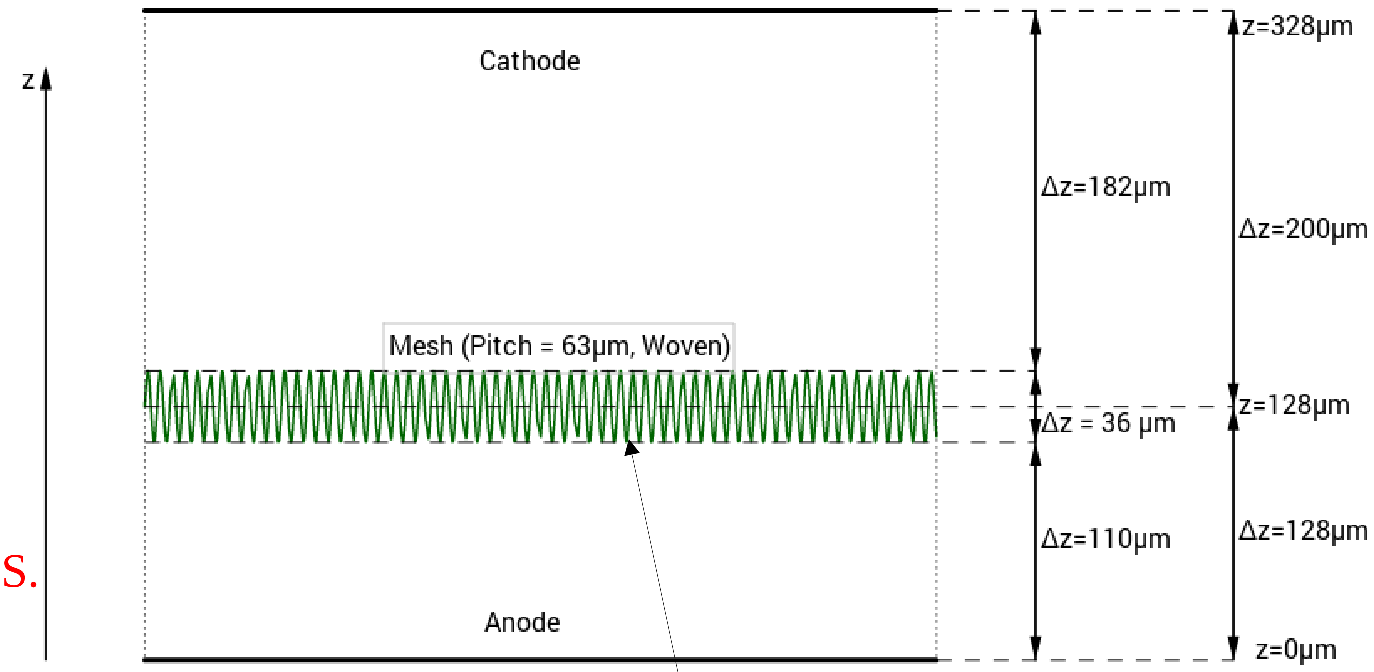

COMPASS gas

(80% Ne + 10% CF_4 + 10% C_2H_6)

1 bar pressure.

Electric field modelled with ANSYS.

Drift gap = 200 μm
Amplification gap = 128 μm
Mesh thickness = 36 μm

Anode Voltage = 450 V → E = 35 kV/cm
Drift Voltage = 300-425 V → E in [15, 21] kV/cm

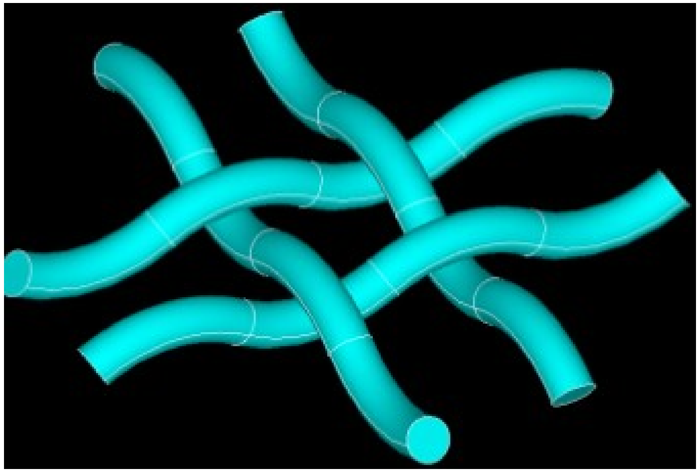

ANSYS

Simulation Cross Sections

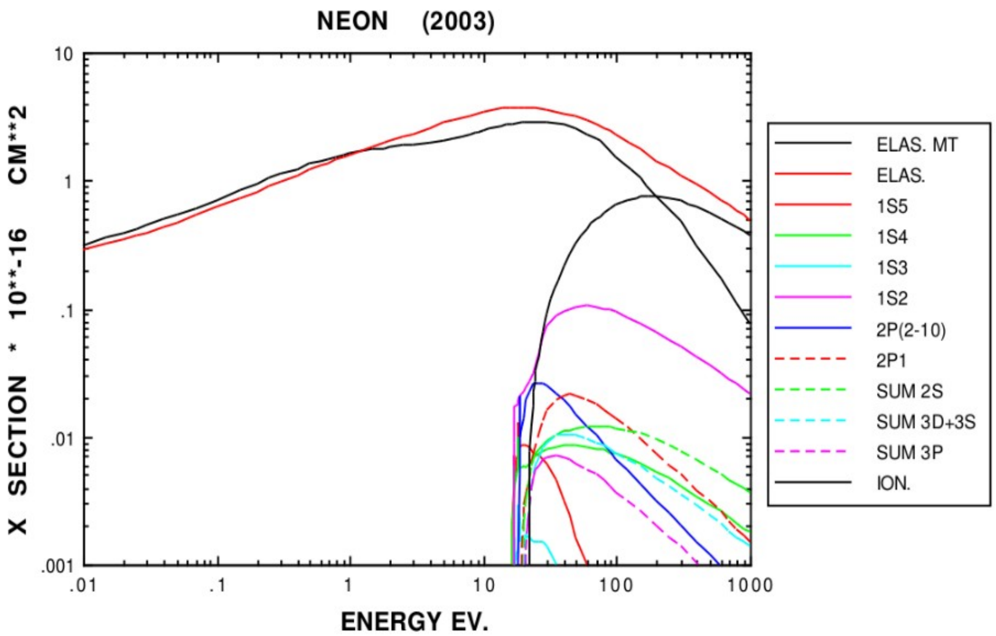

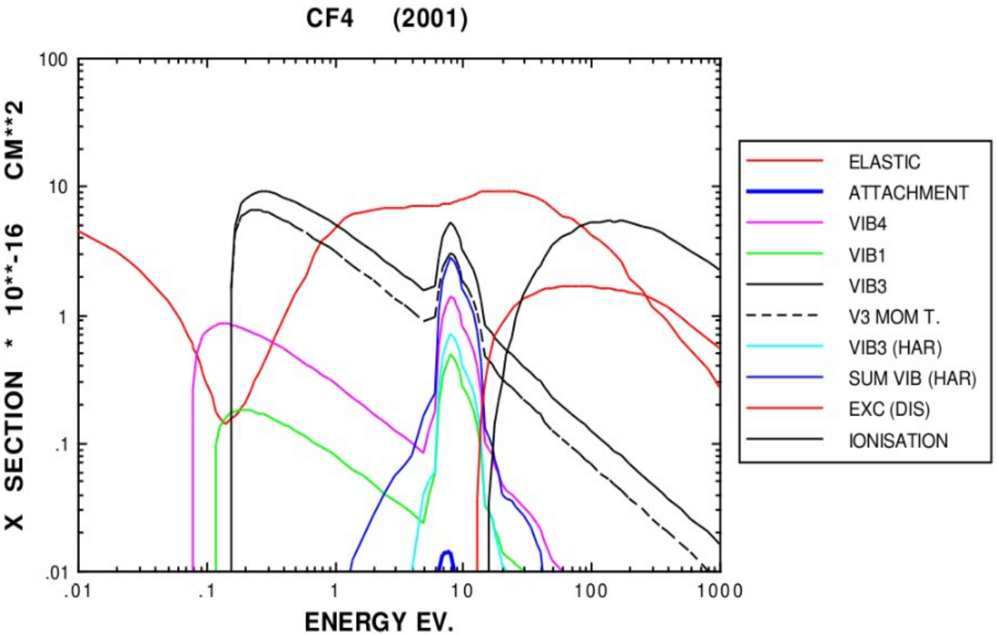

Garfield++ makes use of the cross sections of all interactions between electrons and atoms.

From first principles, it microscopically tracks electrons in the electric field and the gaseous mixture.

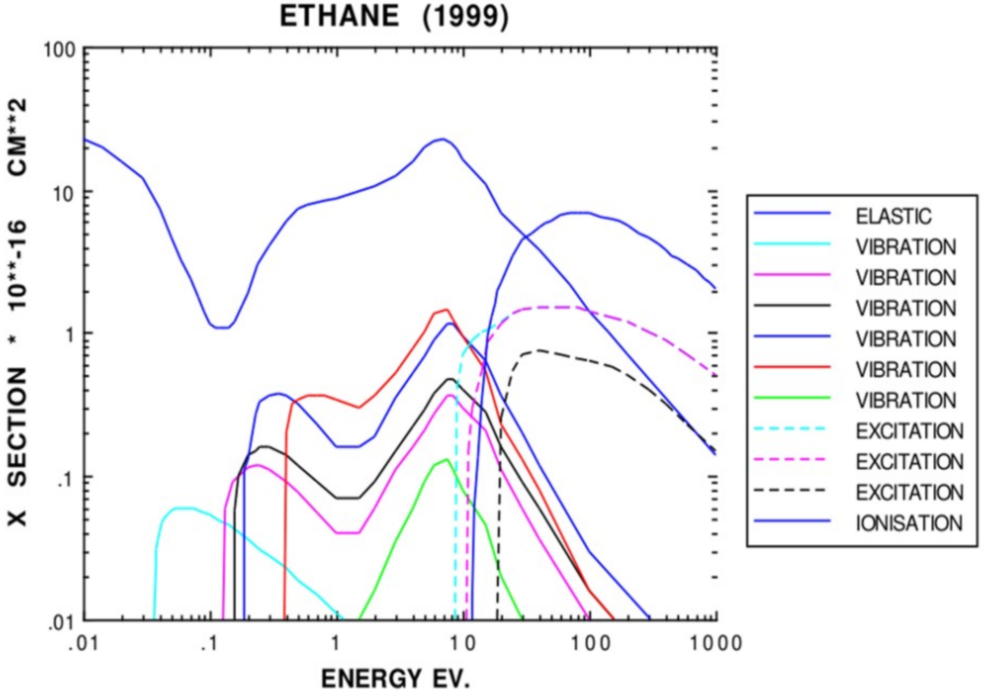

We have observed that the anode does not contribute to the time resolution

To reduce computational time, we separate the simulation in three stages:

1) Simulation until the mesh. Pre-amplification region.

2) Simulation in the amplification region.

3) Electronics consideration.

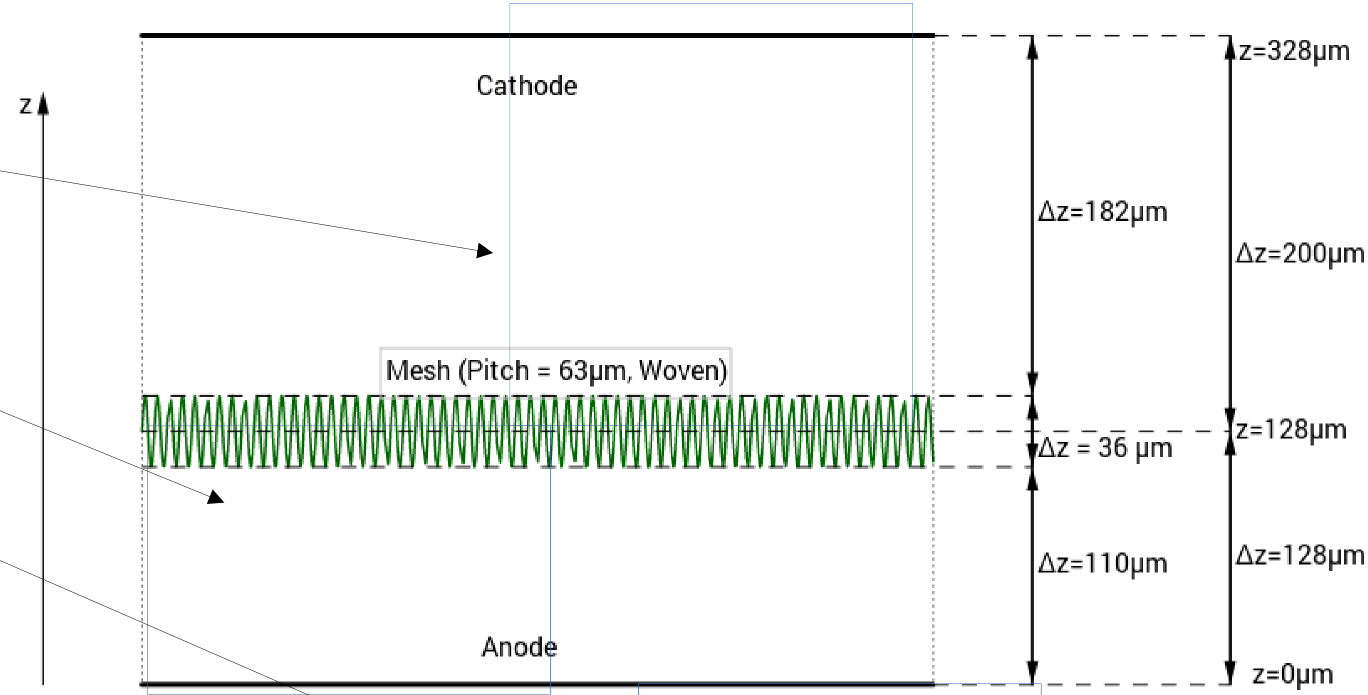

Stage 1 – Pre-amplification region

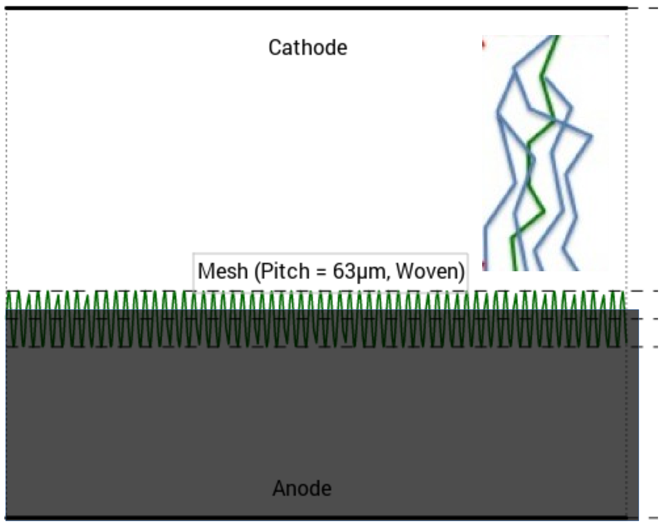

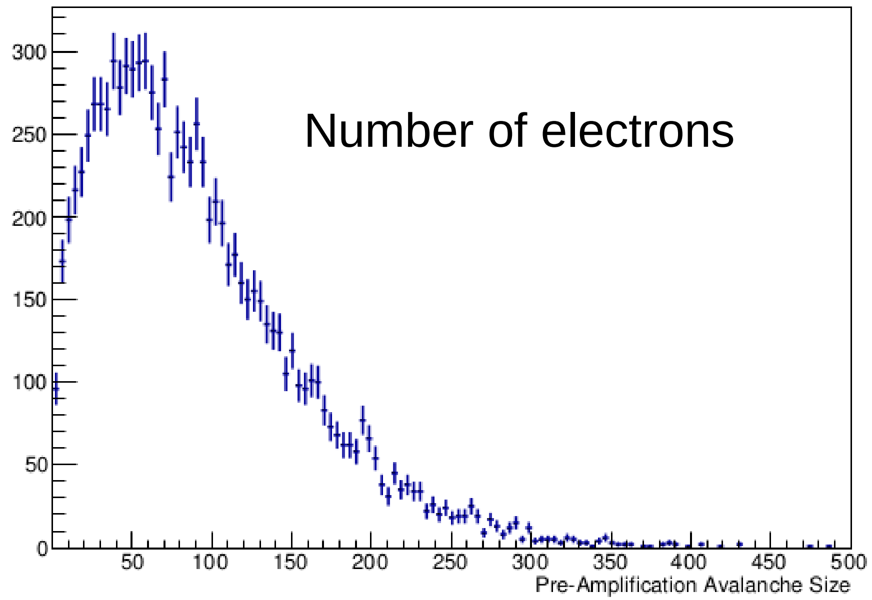

Track an electron beginning from the cathode and its avalanche and record the number of electrons that are passing through the mesh as well as the time at which they pass.

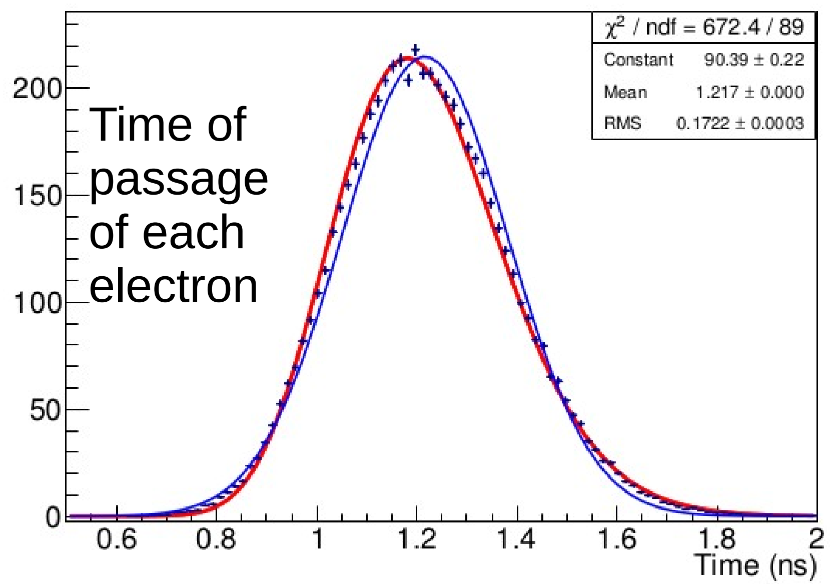

Stage 2 – Amplification Region

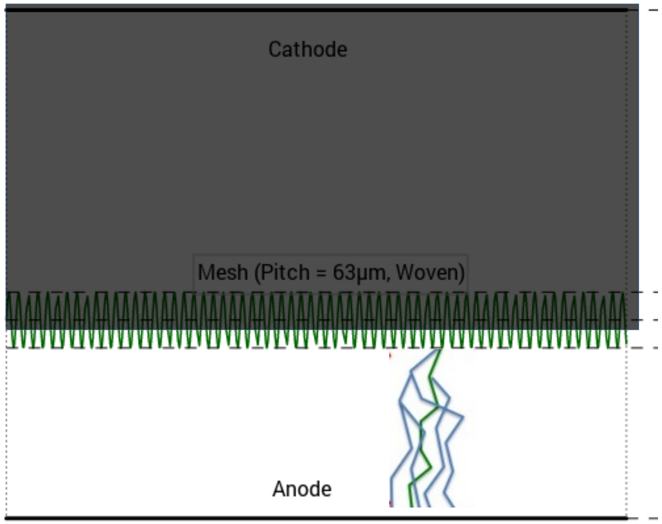

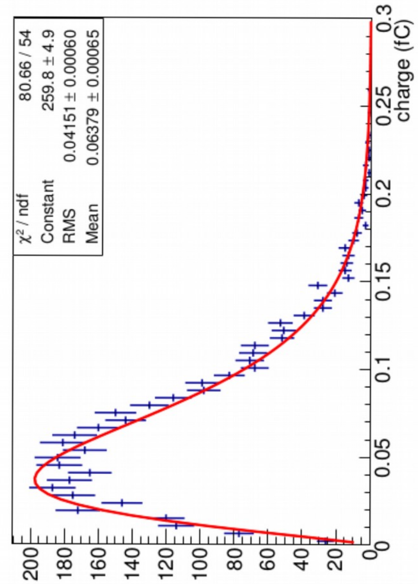

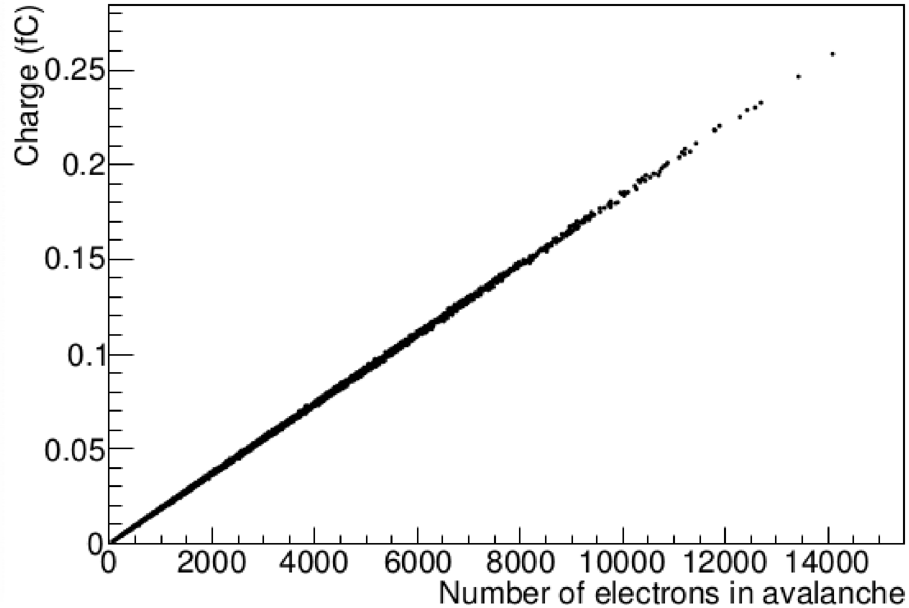

Begin an electron from the mesh and count the number of electrons produced and the charge induced.

Naturally, the charge is proportional to the number of electrons.

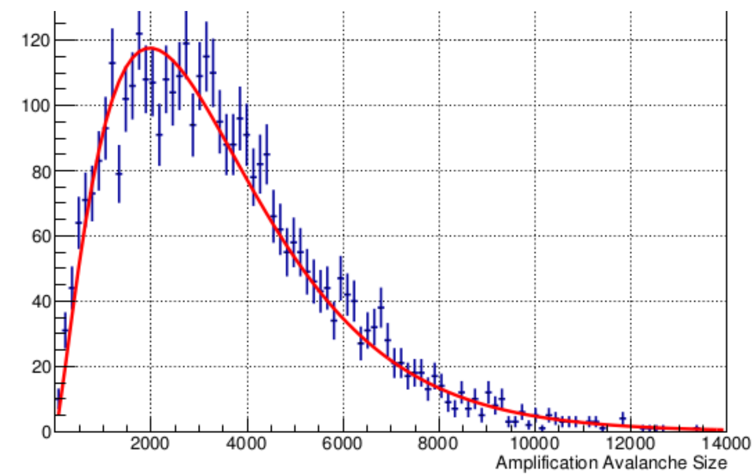

Parameterize with a Polya distribution.

Stage 3 – Electronics

Lab test with pulser

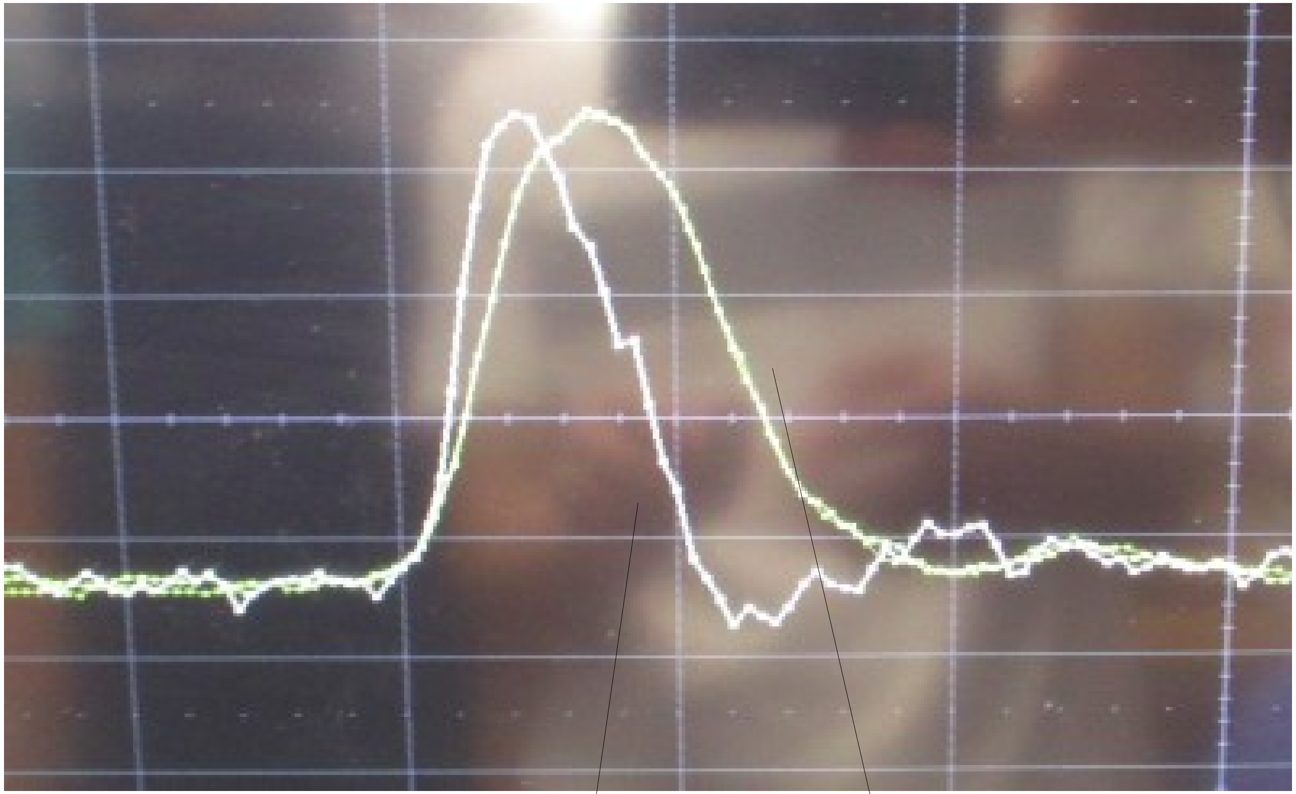

The electronics greatly shape the pulse. Unfortunately, we don't know the transfer function.

input

output (x100)

Stage 3 – Electronics (2)

We search for the shape of the pulse that will be created from a single electron in the region of the anode.

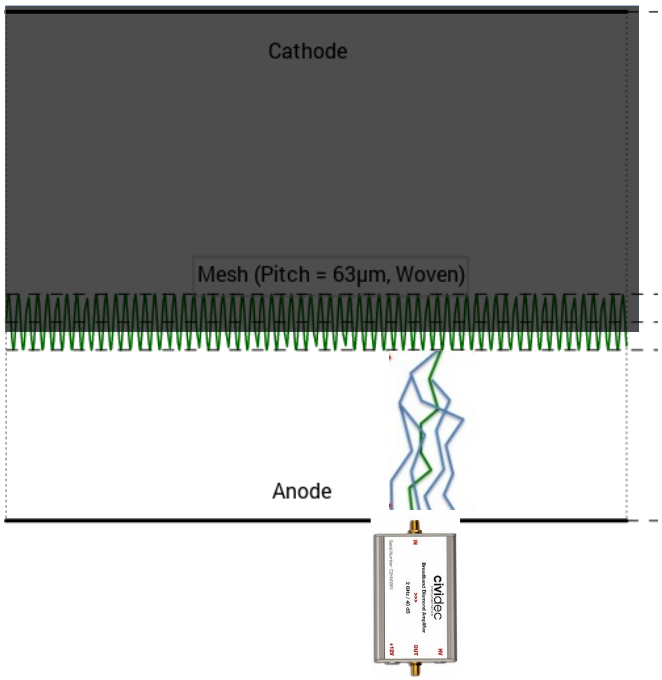

Developed a technique with which we can estimate the waveform of this signal using the experimental data.

We proved that this estimation is made in a statistically consistent and unbiased way by comparing:
a) the convolution of the mean distribution of time of arrivals on the mesh (provided by Garfield++) with a parametric representation of the response
with b) the average waveform that is observed in the experimental data.

parametric representation of the response of an avalanche caused by a single electron entering the amplification region.

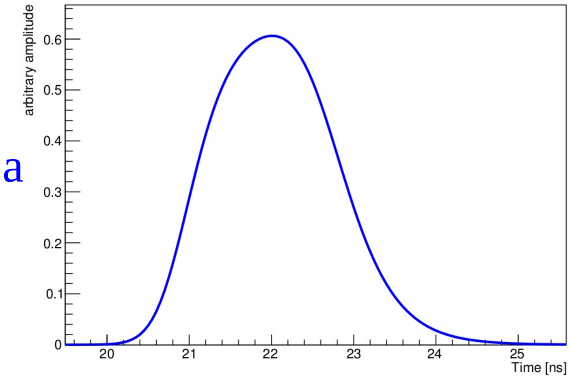

$$f(t; p_0, p_1, p_2, p_3, p_4, p_5, p_6) = \frac{p_0}{(1+e^{-(t-p_1)p_2})^{p_3}} - \frac{p_0}{(1+e^{-(t-p_4)p_5})^{p_6}}$$

Stage 3 – Electronics (3)

Basic steps in the proof:

$$P(\tau_1,...,\tau_k,q_1,...,q_k;k) = R(k)\cdot\prod_{i=1}^{k}\Phi(\tau_i;k)\cdot\prod_{i=1}^{k}G(q_i)$$

$$\bar{S}(t) = \sum_{k=1}^{\infty}R(k)\int_0^{\infty}\cdots\int_0^{\infty}\sum_{i=1}^{k}q_i f(t-\tau_i)\prod_{i=1}^{k}\Phi(\tau_j;k)\cdot\prod_{i=1}^{k}G(q_j)dq_1...dq_k d\tau_1...d\tau_k$$

$$P_{Q_{tot}=Q}(\tau_1,...,\tau_k,q_1,...,q_k;k) = \\ = \frac{\delta\left(Q-\sum_{i=1}^{k}q_i\right)\cdot R(k)\cdot\prod_{i=1}^{k}\Phi(\tau_i;k)\cdot\prod_{i=1}^{k}G(q_i)}{N(k)}$$

where

$$N(k) = \int_0^{\infty}\cdots\int_0^{\infty}\delta\left(Q-\sum_{i=1}^{k}q_i\right)\cdot R(k)\cdot\prod_{i=1}^{k}G(q_i)dq_1...dq_k$$

$$\langle S(t)\rangle_{Q_{tot}=Q} = \\ = \sum_{k=1}^{\infty}R(k)\int_0^{\infty}\cdots\int_0^{\infty}\sum_{i=1}^{k}q_i f(t-\tau_i)\cdot\delta\left(Q-\sum_{i=1}^{k}q_i\right)\cdot \\ \cdot\prod_{j=1}^{k}\Phi(\tau_j;k)\cdot\prod_{j=1}^{k}G(q_j)dq_1...dq_k d\tau_1...d\tau_k$$

$$\langle S(t)\rangle_{Q_{tot}=Q} = \sum_{k=1}^{\infty}R(k)\sum_{i=1}^{k}\int_0^{\infty}f(t-\tau_i)\Phi(\tau_i;k)d\tau_i\cdot \\ \cdot\int_0^{\infty}\cdots\int_0^{\infty}q_i\cdot\delta\left(Q-\sum_{i=1}^{k}q_i\right)\cdot\prod_{j=1}^{k}G(q_i)dq_1...dq_k$$

$$\langle q_i\rangle_{Q=\sum_{j=1}^{k}q_j} = \frac{\int_0^{\infty}\cdots\int_0^{\infty}q_i\cdot\delta\left(Q-\sum_{i=1}^{k}q_i\right)\cdot\prod_{j=1}^{k}G(q_i)dq_1...dq_k}{N(k)}$$

$$\langle S(t)\rangle_{Q_{tot}=Q} = \sum_{k=1}^{\infty}R(k)N(k)\sum_{i=1}^{k}\int_0^{\infty}f(t-\tau_i)\Phi(\tau_i;k)d\tau_i\cdot \\ \cdot\int_0^{\infty}\cdots\int_0^{\infty}\frac{q_i\cdot\delta\left(Q-\sum_{i=1}^{k}q_i\right)\cdot\prod_{j=1}^{k}G(q_i)}{N(k)}dq_1...dq_k$$

$$\langle S(t)\rangle_{Q_{tot}=Q} = \sum_{k=1}^{\infty}R(k)N(k)\cdot\sum_{i=1}^{k}\langle q_i\rangle_{Q=\sum_{j=1}^{k}q_j}\int_0^{\infty}f(t-\tau_i)\Phi(\tau_i;k)d\tau_i$$

$$\int_0^{\infty}f(t-\tau_i)\Phi(\tau_i;k)d\tau_i = \int_0^{\infty}f(t-\tau)\Phi(\tau;k)d\tau$$

$$\langle S(t)\rangle_{Q_{tot}=Q} = \sum_{k=1}^{\infty}R(k)N(k)\int_0^{\infty}f(t-\tau)\Phi(\tau;k)d\tau\sum_{i=1}^{k}\langle q_i\rangle_{Q=\sum_{j=1}^{k}q_j}$$

$$= Q\sum_{k=1}^{\infty}R(k)N(k)\int_0^{\infty}f(t-\tau)\Phi(\tau;k)d\tau$$

$$= Q\int_0^{\infty}f(t-\tau)\left\{\sum_{k=1}^{\infty}R(k)N(k)\Phi(\tau;k)\right\}d\tau$$

$$\langle\Phi(\tau)\rangle_{Q_{tot}=Q} = \sum_{k=1}^{\infty}R(k)N(k)\Phi(\tau;k)$$

Stage 3 – Electronics (4)

$$\frac{\langle S(t)\rangle_{Q_{tot}=Q}}{Q} = \int_0^\infty f(t-\tau)\,\langle\Phi(\tau)\rangle_{Q_{tot}=Q}\,d\tau$$

Average waveform / Its charge = Single amplification avalanche response * (convolution) Mean time of arrival distribution

(Known experimentally) (known in the simulation)

$$f(t;p_0,p_1,p_2,p_3,p_4,p_5,p_6) = \frac{p_0}{(1+e^{-(t-p_1)p_2})^{p_3}} - \frac{p_0}{(1+e^{-(t-p_4)p_5})^{p_6}}$$

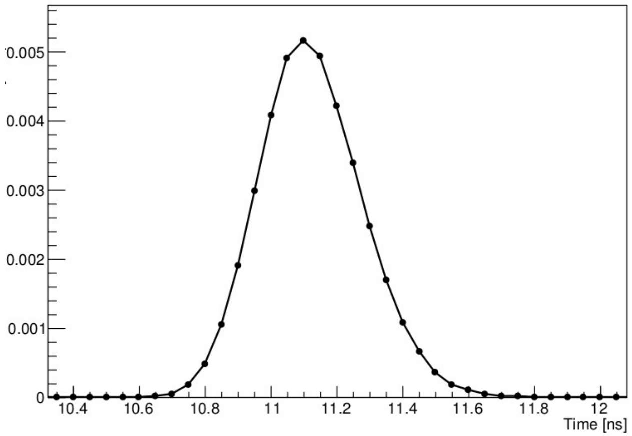

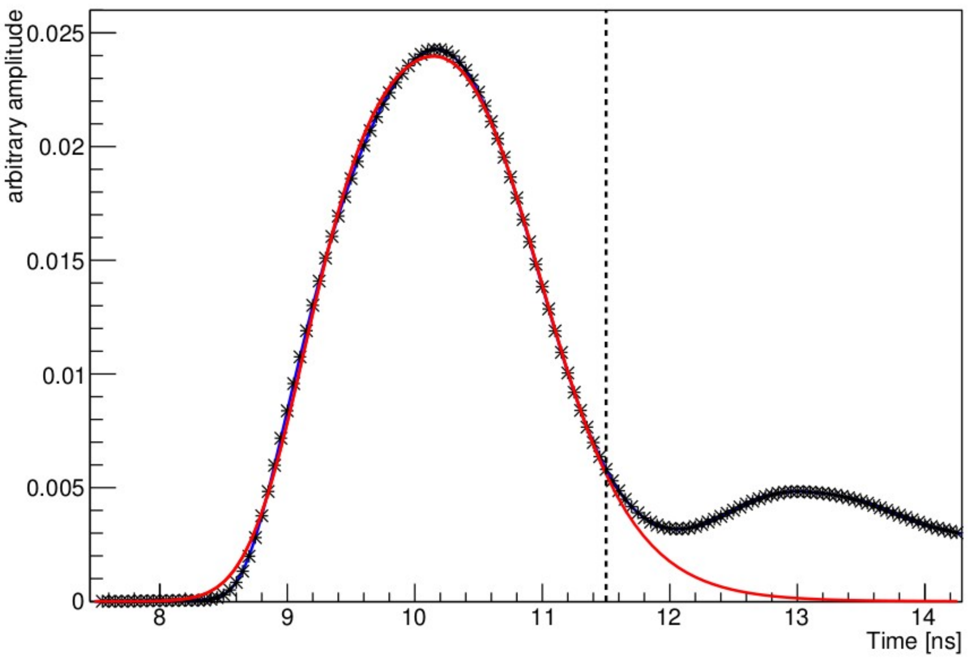

Fit to the experiment to find p0, p1,…,p6.

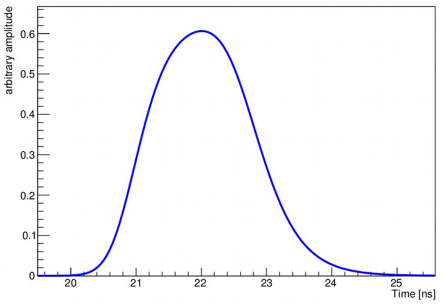

Waveform Generation

N electrons pass through the mesh at times τ1, τ2, …, τN

Every electron will contribute with a pulse **f(t)** **shifted by the corresponding time,** where the size is randomly sampled from the Polya parameterization of the amplification

$$S(t) = \sum_{i=1}^{N} q_i \cdot f(t - \tau_i)$$

Generated pulses are treated the same as the experimental data.

Before continuing, it should be checked that the average shape of the waveforms are the same.

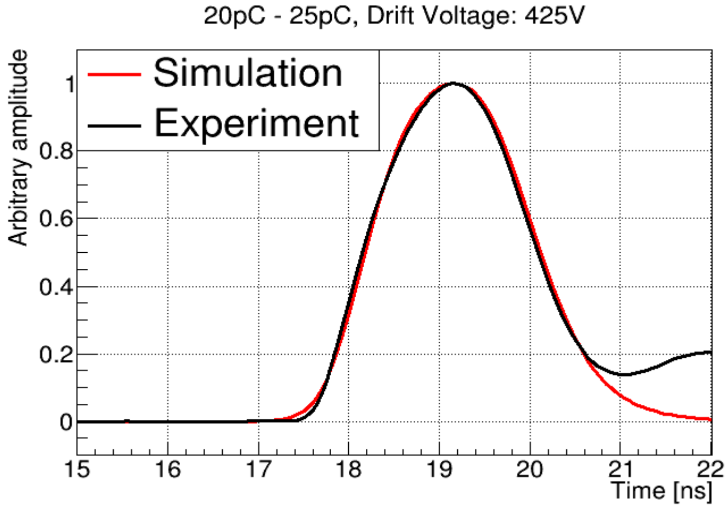

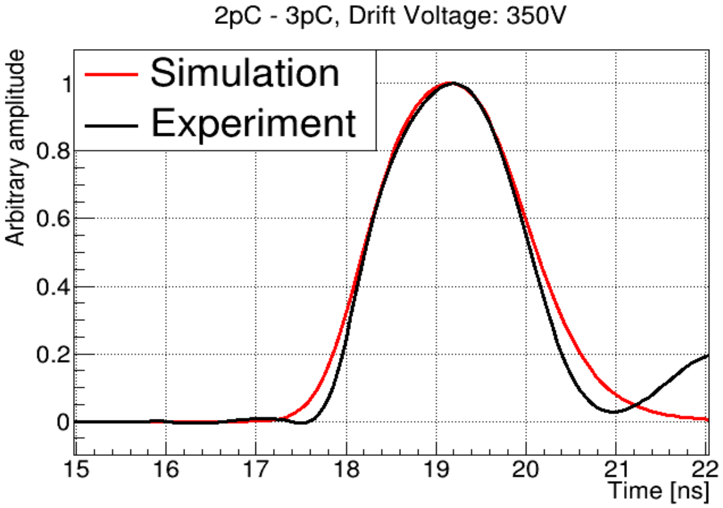

Through this procedure, the absolute gain of the electronics is lost. We scale the charge distribution of the simulation to the experiment and find the scaling factor. Independently of the drift voltage, the scaling factor should be the same without extra fine-tuning.
But…

Experiment
Simulation

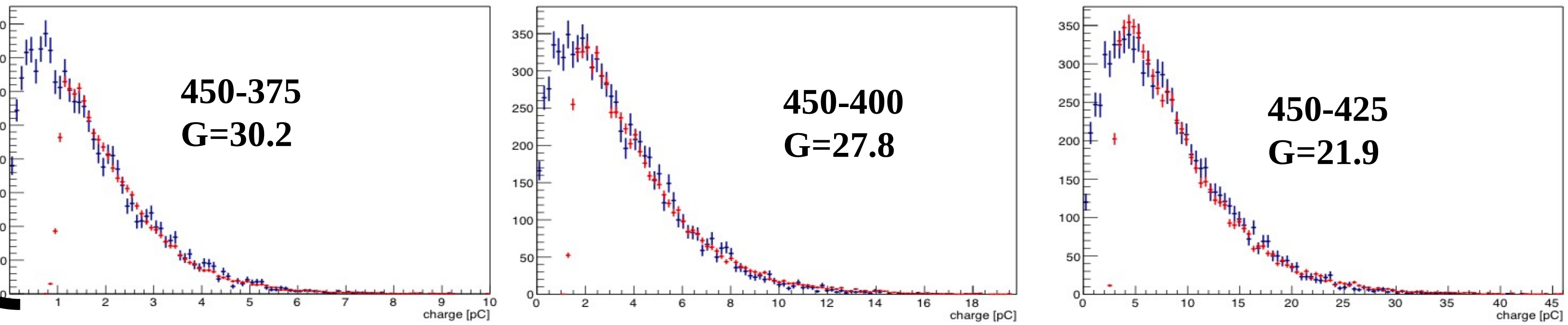

In Garfield++ the interactions between ions and the gas are not microscopically included. Ne has excitation states in energy levels that are higher than the ionization threshold of C2H6 and can ionize it directlv. The collection of such interactions are called Penning transfers.

$$Ne^* + C_2H_6 \rightarrow Ne + C_2H_6^+ + e^-$$

It can be included through a Penning transfer rate which describes the probability for an excitation state to ionize another molecule.

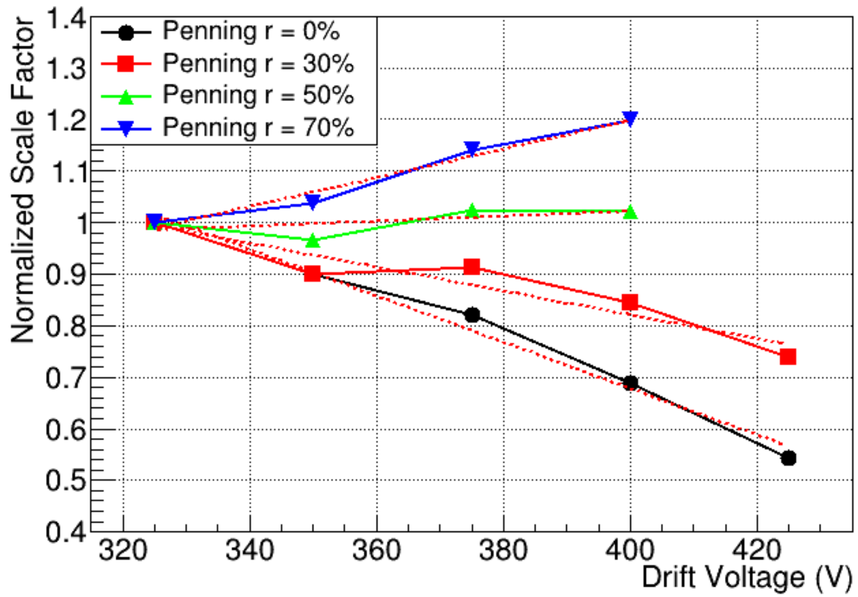

For approximately $r \approx 50\%$, the scale factor does not change with the drift voltage.

Analysis of Simulation

By including “naive” electronic noise...

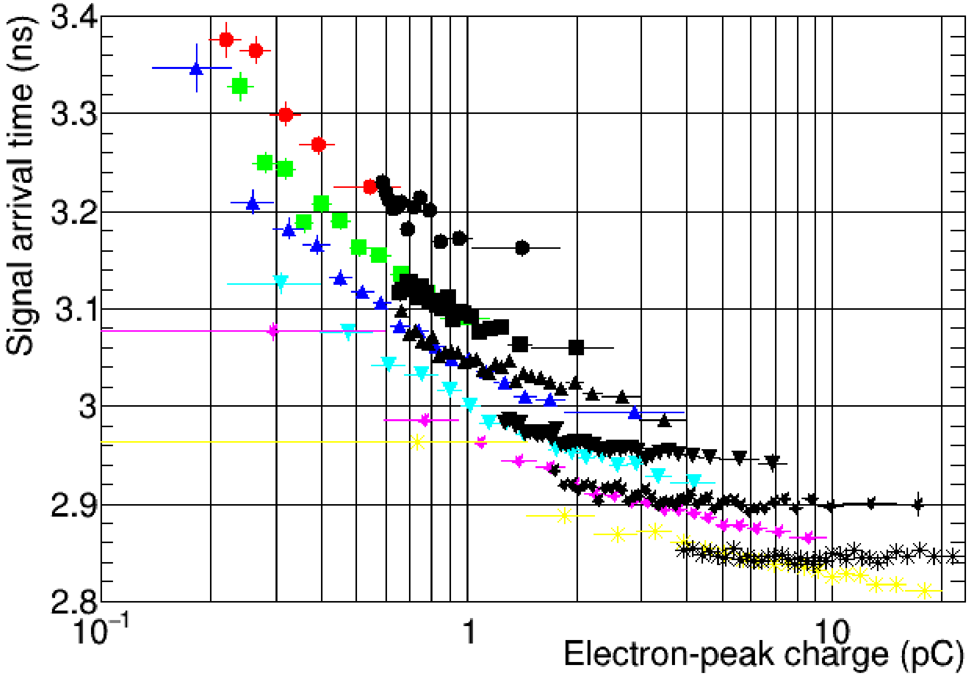

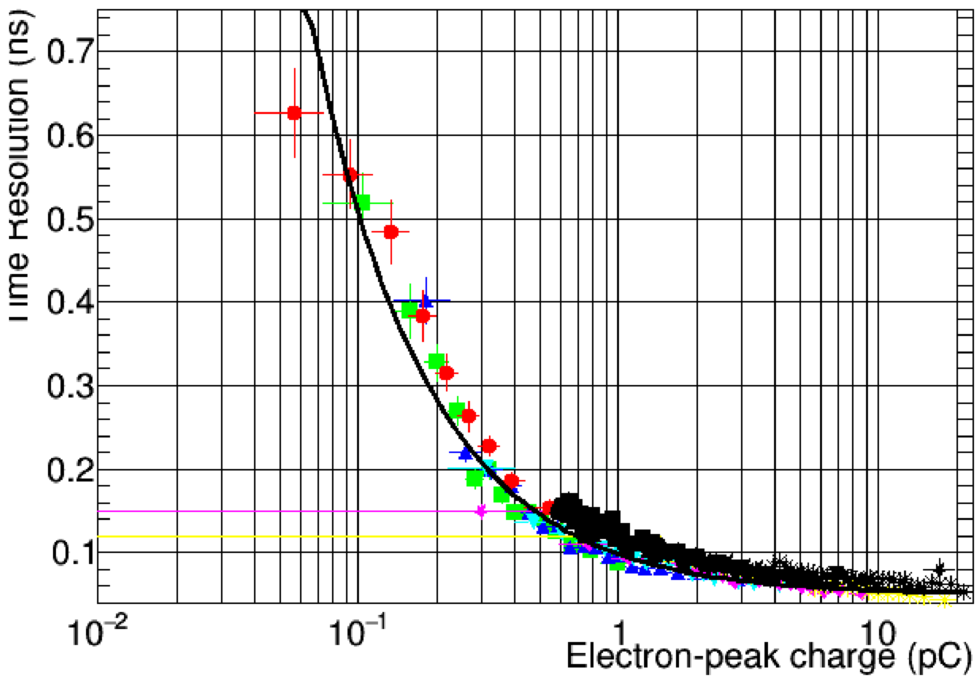

The agreement looks promising and it can become even better with some extra fine tuning.

However, the reproduction of the experimental observations was the not the purpose.

Reminder:

1.) Large signals arrive faster than smaller ones.

2.) The shape of SAT versus the electron peak charge does not change with the Drift Voltage.

3.) Time resolution versus the electron peak charge does not change with the Drift Voltage.

experimental Average Waveforms

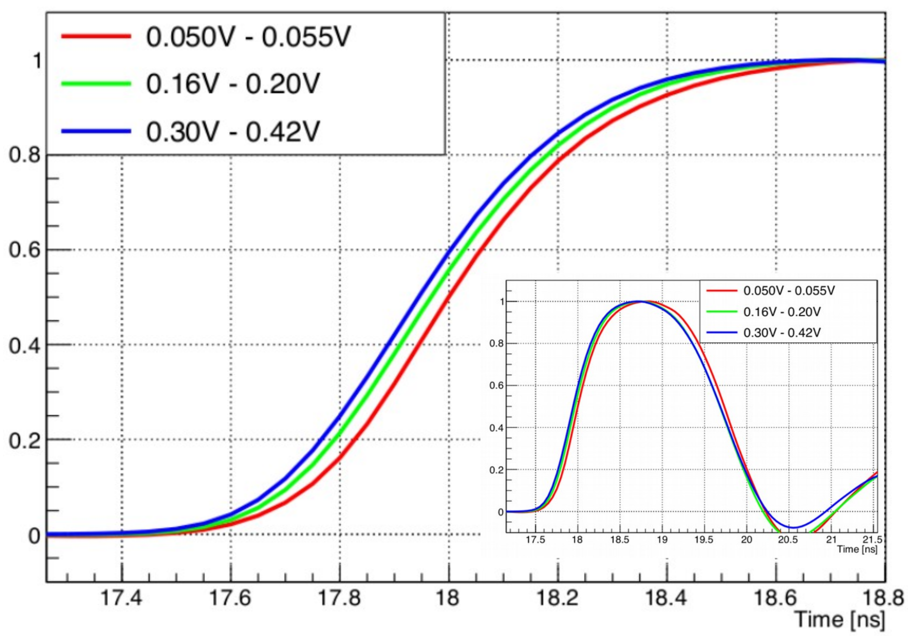

simulated Average Waveforms

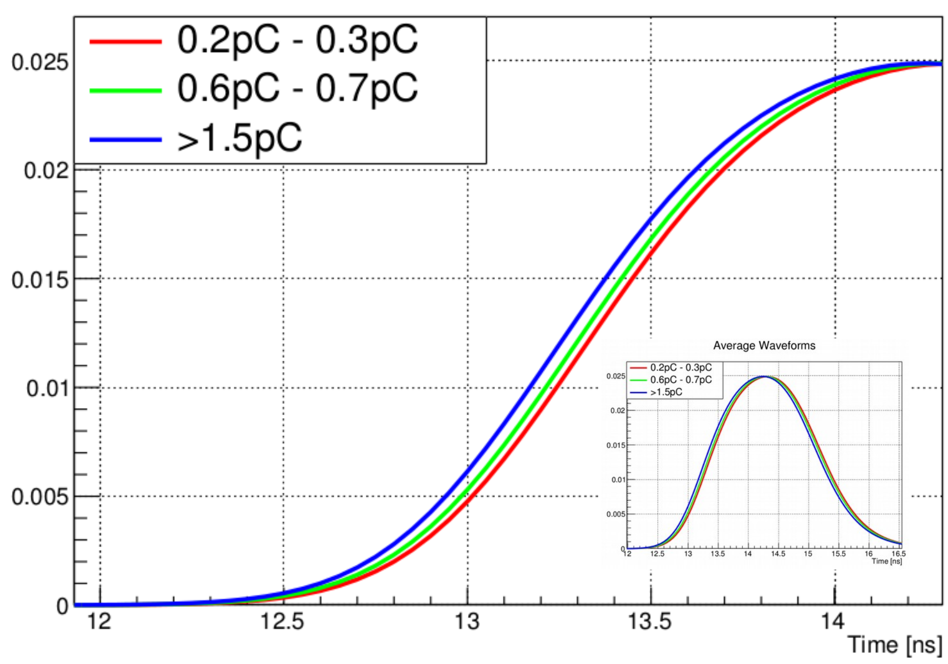

The only reason that a slewing/time-walk effect would be observed is if the leading edge of the waveform was changing shape with its size.

Instead, both experiment and simulation the average leading edge of the signal looks “displaced”.

This is an indication that there exists a physical process in the detector that produces this effect.

Macroscopic → Microscopic

After many tests,
we found that the Signal Arrival Time that is measured with constant fraction discrimination, corresponds to the mean time that the avalanche's electrons transmit through the mesh.

$$t_i = \frac{\tau_1 + \tau_2 + \ldots + \tau_N}{N}$$

For each simulated event, both are known.

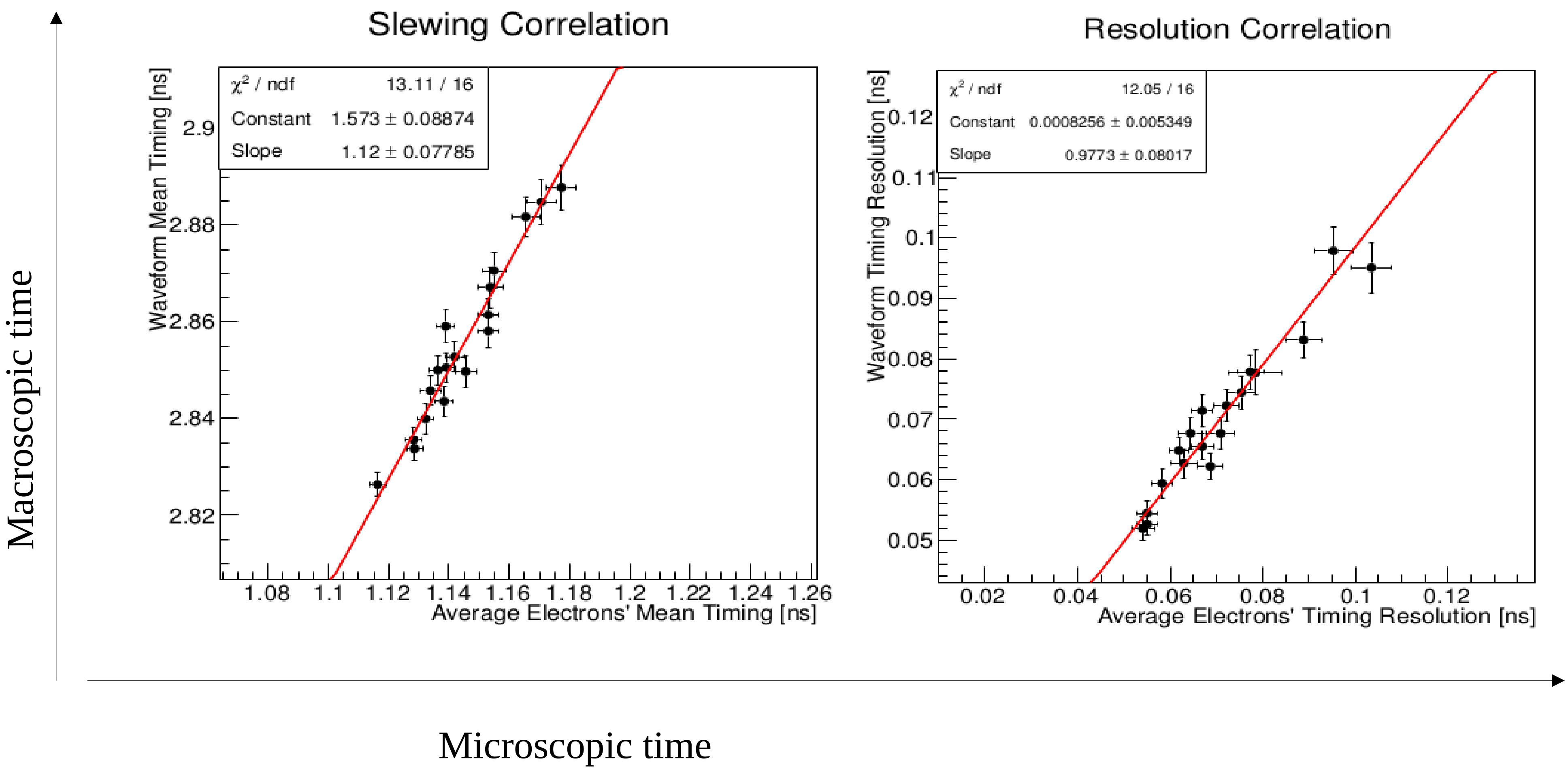

Microscopic Study

We choose another variable which goes closer to the microscopic picture of the signal formation.

The length of the avalanche D.
(from the point of the first ionization until the mesh).

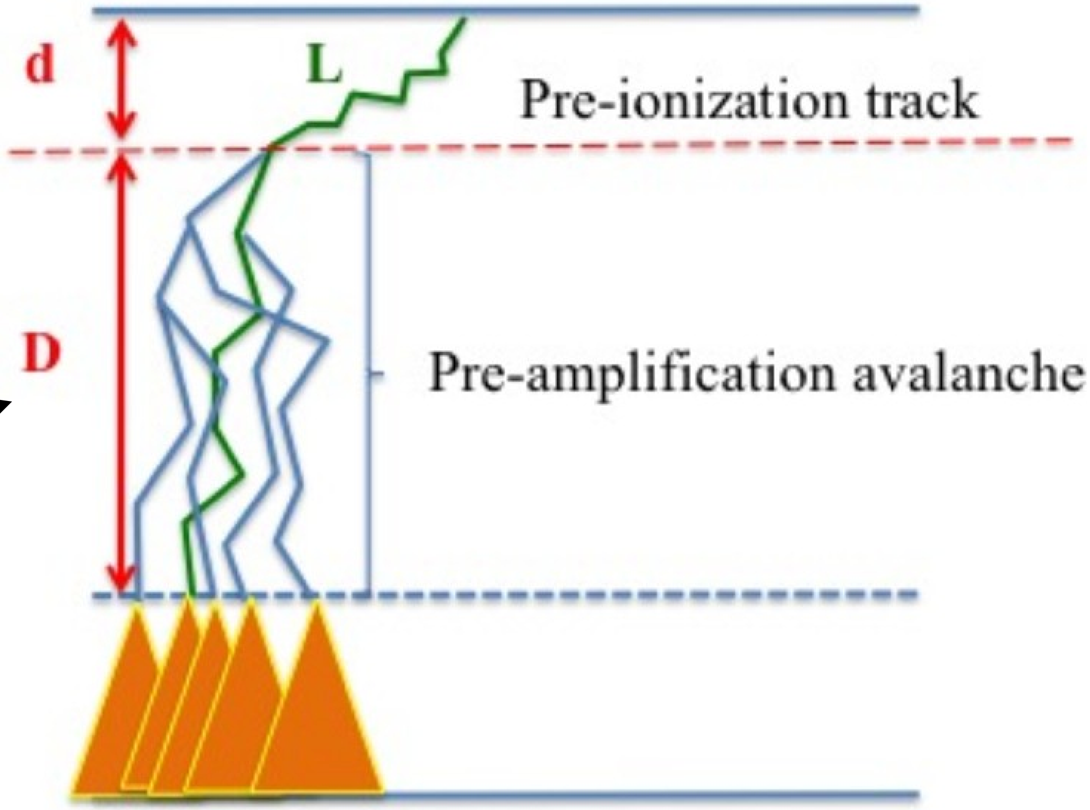

Microscopic Study

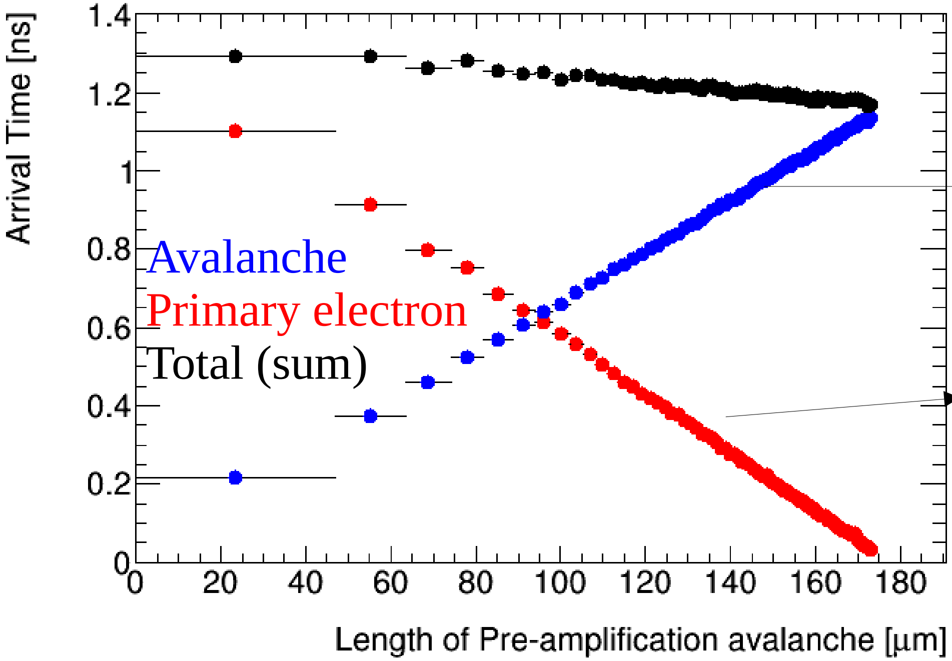

$$slope = \frac{1}{v} = \frac{1}{153.94\,\mu m/ns}$$

$$slope = \frac{1}{v} = \frac{1}{134.34\,\mu m/ns}$$

The electron before the ionization moves slower than the avalanche (after the ionization).

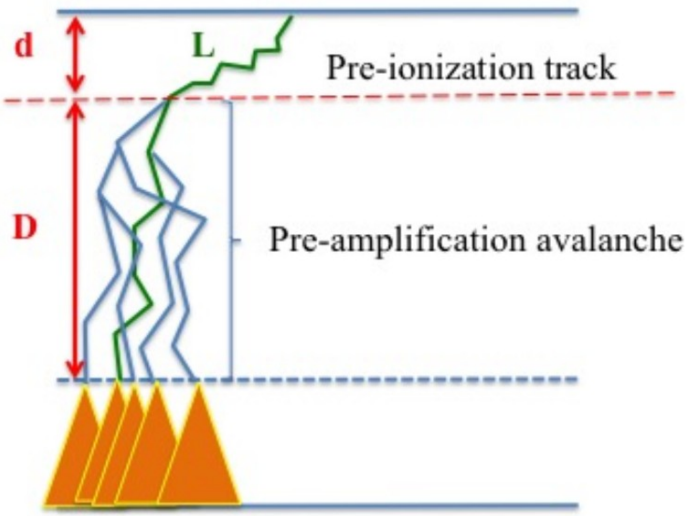

By definition, the primary electron before the first ionization, can't have ionized.

In contrast, after the first ionization it is free to continue ionizing.

Phenomenological Explanation

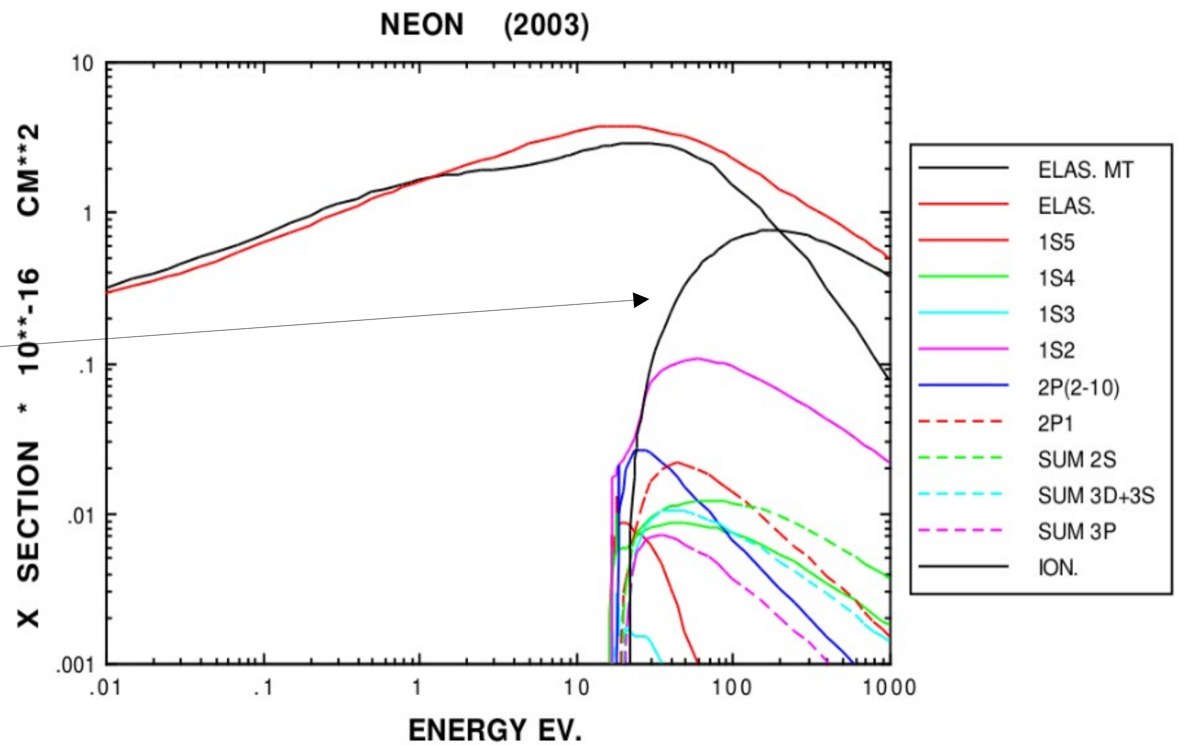

Before ionizing, the electron cannot participate in the **inelastic** cross section of ionization and cannot lose energy this way.

This leads to a very slightly increased mean energy (and instant velocity) distribution for the electrons. **However, when a faster electron scatters backwards, the electric field needs more time to recover a forward direction of motion.**

This is also how the addition of quenching molecules in the gas mixture makes the drift velocity larger.

~~1.) Large signals arrive faster than smaller ones.~~

2.) The shape of SAT versus the electron peak charge does not change with the Drift Voltage.

3.) Time resolution versus the electron peak charge does not change with the Drift Voltage.

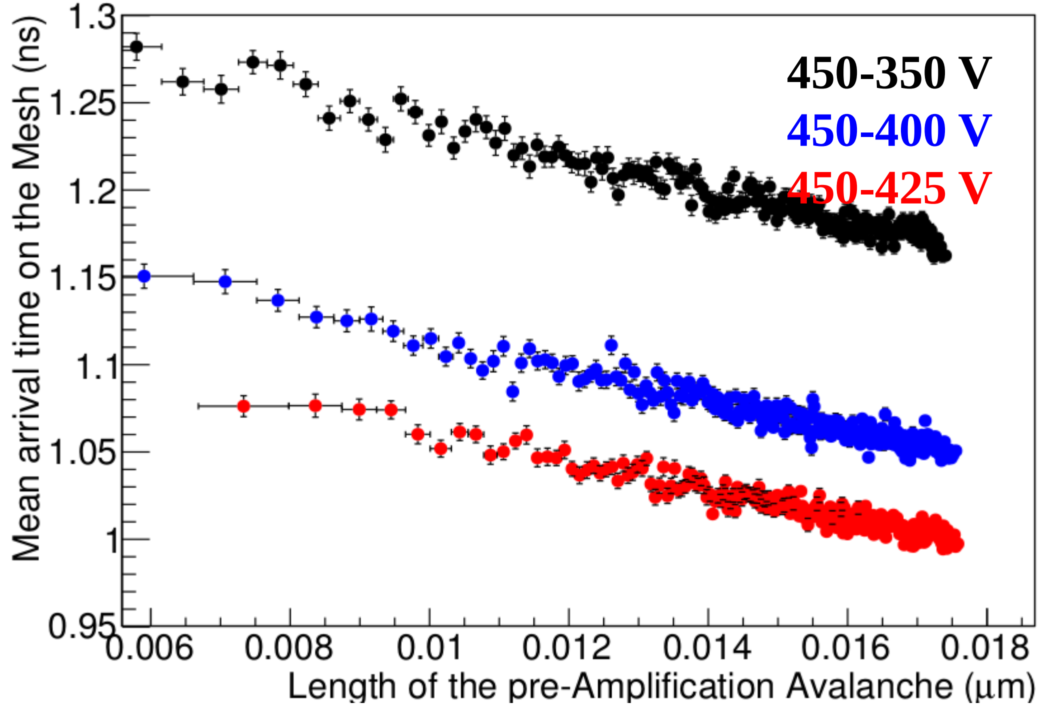

Fig: SAT vs **length of pre-amplification avalanche**

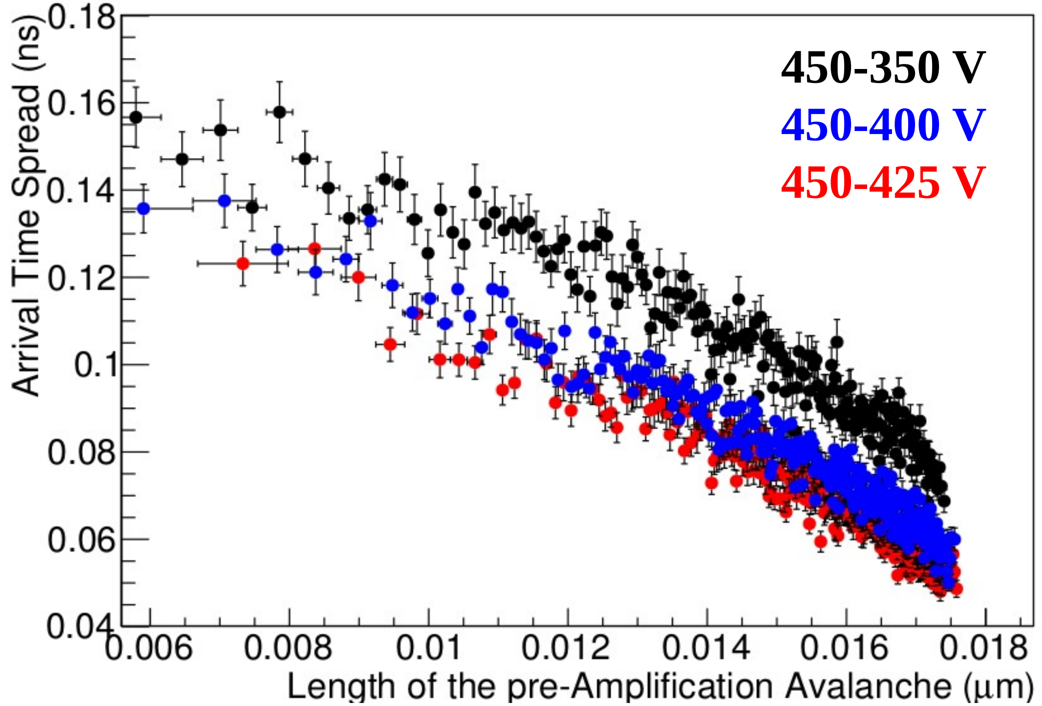

Fig: Resolution vs **length of pre-amplification avalanche**

Obviously, diffusion and the length of the avalanche depends on the electric field. For example, the time spread (right) depends on the applied voltage on the cathode.

Avalanches with the same length are not producing the same number of electrons if the electric field is different.

However, the length of the avalanche is not observable.
To compare with experimental data, the simulation must be re-parameterized in terms of the number of electrons (passing through the mesh).

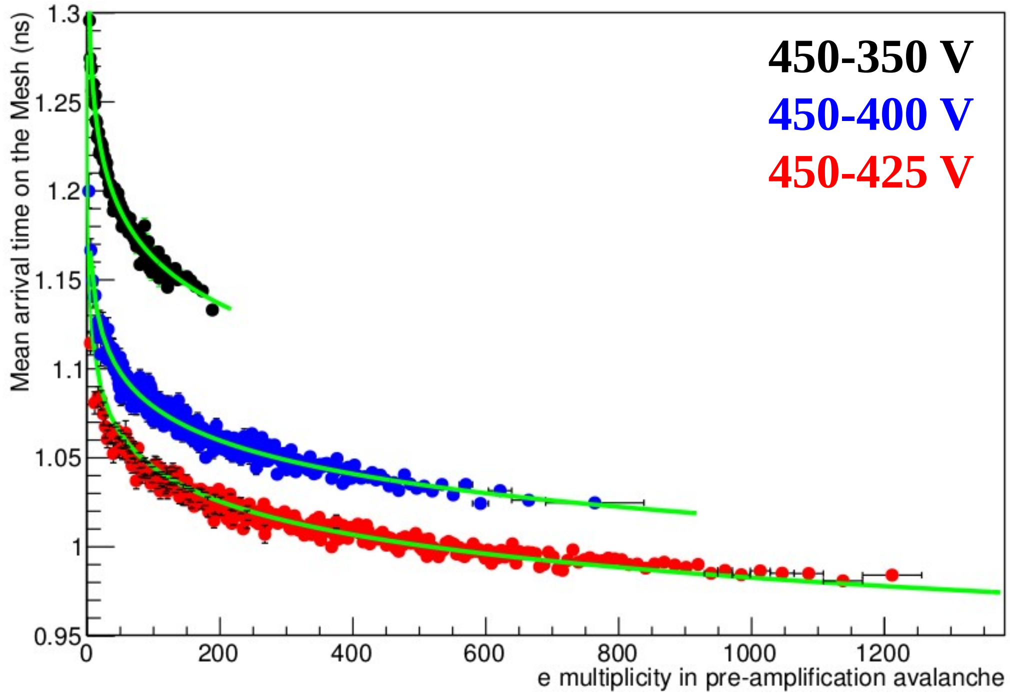

Fig: SAT vs **secondary electrons' multiplicity of pre-amplification avalanche**

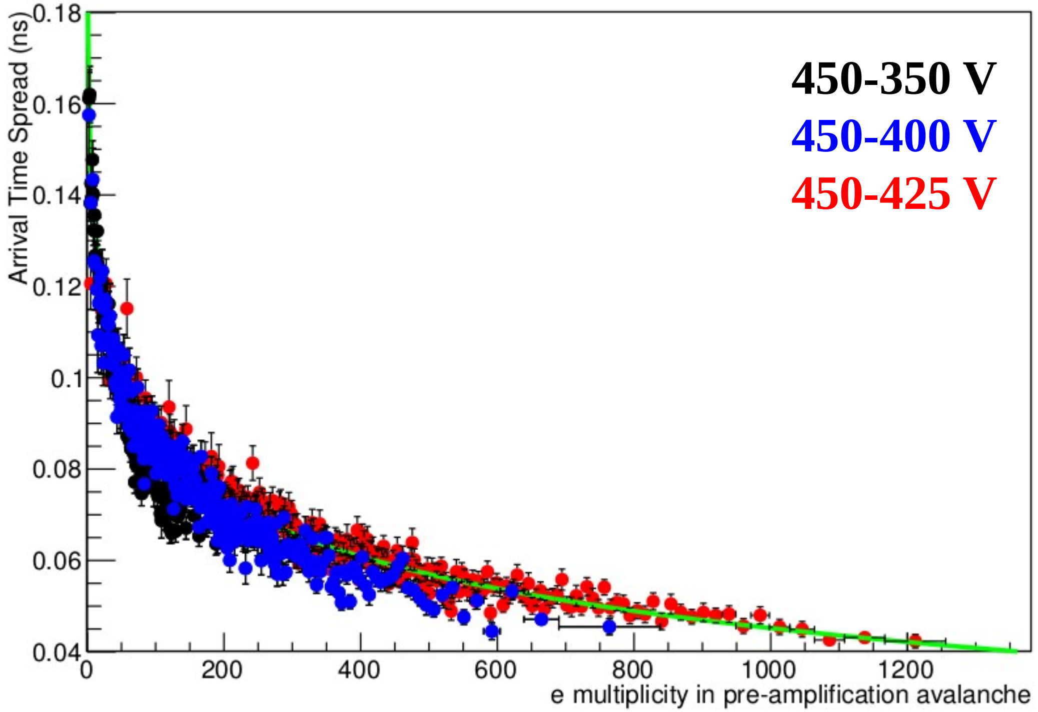

Fig: Resolution vs **secondary electrons' multiplicity of pre-amplification avalanche**

By reparameterizing in terms of the number of electrons which is proportional to the size of the waveform.

By examining the different drift voltage settings, the simulation indeed predicts that the timing characteristics as a function of the number of electrons are independent.

To aid in our understanding and to go deeper into the physics of PICOSEC, we shall build a simple one-dimensional model.

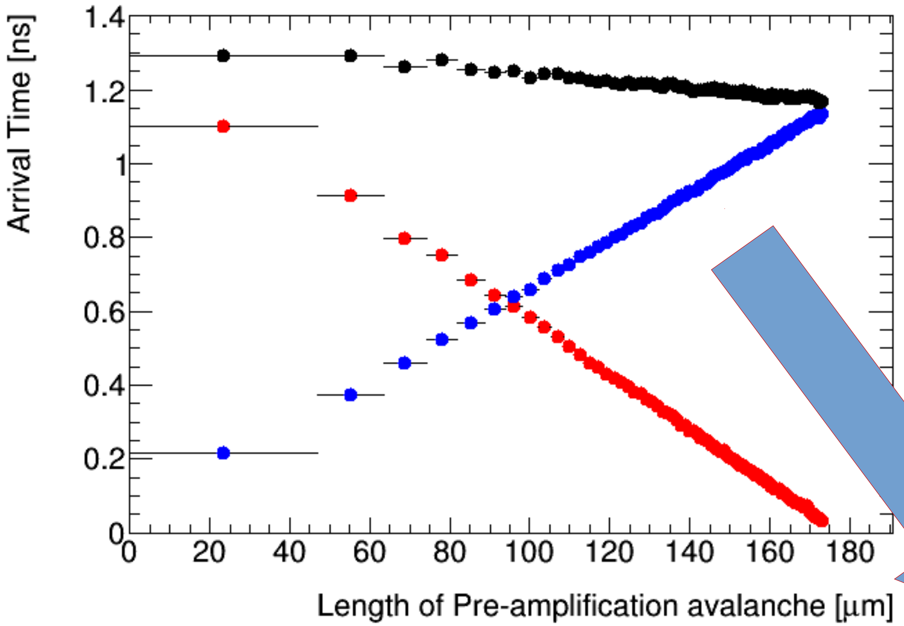

Subtract expected time based on constant drift velocity and reparameterize in terms of number of electrons.

There is a clear dependence on number of electrons.

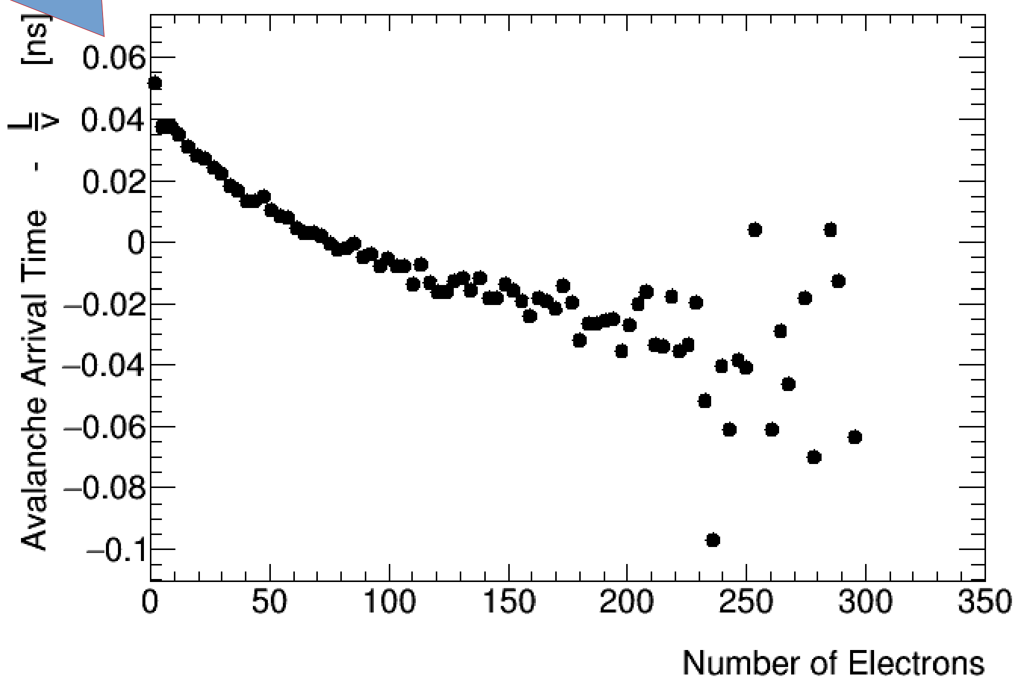

To describe avalanche gain spectra, W. Legler postulated that there exists a characteristic distance which a newly freed electron needs to travel before it can ionize again.

Inspired by this model, we consider a characteristic time which electrons jump forward after ionizing collisions.

Each time an electron ionizes, it jumps forward in time time with an amount equal to ρ_1.

Each time an electron is "created", it jumps forward in time time with an amount equal to ρ_2.

PDF to observe avalanche of length L: $R(L;a) = \frac{ae^{aL}}{e^{ax_2} - e^{ax_1}}$ *where* $L \in [x_1, x_2]$

and a is the first Townsed coefficient.

PDF to observe avalanche with n electrons: $P(n;q,\theta) = \frac{1}{q} \frac{(\theta+1)^{\theta+1}}{\Gamma(\theta+1)} \left(\frac{n}{q}\right)^{\theta} e^{(\theta+1)\frac{n}{q}}$

Mean n grows exponentially with L: $q(L;a_{eff}) = 2 \cdot e^{a_{eff} L}$

Probability for an avalanche to have length L and n electron: $G(L|n)\,dL = \frac{P(n;2 \cdot e^{a_{eff}L},\theta) \cdot R(L;a)}{\int_{x_1}^{x_2} P(n;2 \cdot e^{a_{eff}L},\theta) \cdot R(L;a)} dL$

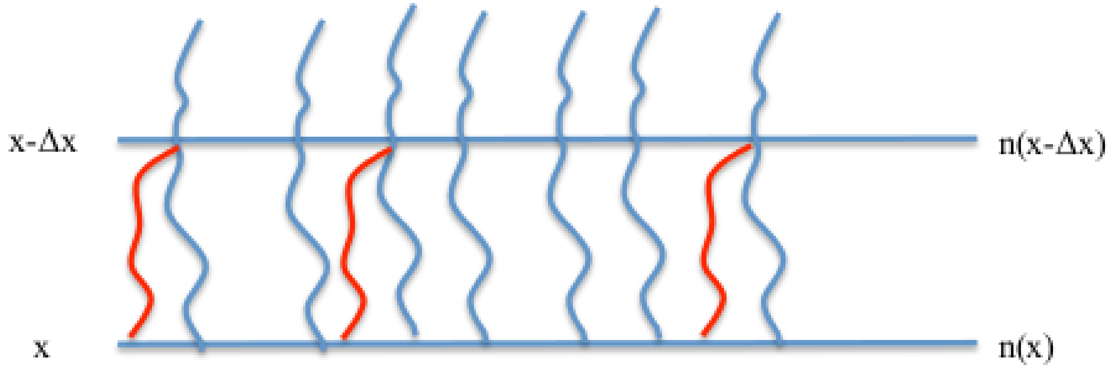

$$T(x) = \frac{1}{n(x)} \sum_{k=1}^{n(x)} t_k(x)$$

$$n(x)T(x) - n(x-\Delta x)T(x-\Delta x) = \sum_{k=1}^{n(x)} t_k(x) - \sum_{k=1}^{n(x-\Delta x)} t_k(x-\Delta x) \quad (1)$$

$$\left.\begin{aligned} &\sum_{k=1}^{n(x)} t_k(x) = \sum_{k=1}^{n(x-\Delta x)} t_k(x-\Delta x) + \sum_{k=1}^{n(x-\Delta x)} \underbrace{\left[t_k(x) - t_k(x-\Delta x)\right]}_{\Delta t_k} + \sum_{k=n(x-\Delta x)}^{n(x)} \tau_k^f(x) \\ &\textit{where } f \textit{ is the father}: \quad f \in \{1,2,3,\ldots n(x-\Delta x)\} \end{aligned}\right\} (2)$$

$$\sum_{k=n(x-\Delta x)}^{n(x)} \tau_k^f(x) = \frac{n(x)-n(x-\Delta x)}{n(x-\Delta x)} \sum_{k=1}^{n(x-\Delta x)} \tau_k(x) = \frac{\Delta n}{n(x-\Delta x)} \sum_{k=1}^{n(x-\Delta x)} \left[t_k(x-\Delta x) + \Delta\tau_\kappa\right] \quad (3)$$

Substituting (2) *and* (3) int*o* (1)

$$n(x)T(x) - n(x-\Delta x)T(x-\Delta x) = \sum_{k=1}^{n(x-\Delta x)} t_k(x-\Delta x) + \sum_{k=1}^{n(x-\Delta x)} \Delta t_k + \frac{\Delta n}{n(x-\Delta x)} \sum_{k=1}^{n(x-\Delta x)} \left[t_k(x-\Delta x) + \Delta\tau_\kappa\right] - \sum_{k=1}^{n(x-\Delta x)} t_k(x-\Delta x)$$

$$= \sum_{k=1}^{n(x-\Delta x)} \Delta t_k + \frac{\Delta n}{n(x-\Delta x)} \sum_{k=1}^{n(x-\Delta x)} \left[t_k(x-\Delta x) + \Delta\tau_\kappa\right] \quad (4)$$

$$\left.\begin{aligned} &n(x)T(x) - n(x-\Delta x)T(x-\Delta x) - \frac{\Delta n}{n(x-\Delta x)} \sum_{k=1}^{n(x-\Delta x)} t_k(x-\Delta x) = \sum_{k=1}^{n(x-\Delta x)} \Delta t_k + \frac{\Delta n}{n(x-\Delta x)} \sum_{k=1}^{n(x-\Delta x)} \left[\Delta\tau_\kappa\right] \\ &n(x)T(x) - n(x)T(x-\Delta x) = \sum_{k=1}^{n(x-\Delta x)} \Delta t_k + \frac{\Delta n}{n(x-\Delta x)} \sum_{k=1}^{n(x-\Delta x)} \left[\Delta\tau_\kappa\right] \end{aligned}\right\} \quad (5)$$

averaging (5) *for all time developments under the condition that the multiplicities are* $n(x)$ *and* $n(x-\Delta x)$

$$\boxed{n(x)\langle T(x)\rangle - n(x)\langle T(x-\Delta x)\rangle = \sum_{k=1}^{n(x-\Delta x)} \langle \Delta t_k \rangle + \frac{\Delta n}{n(x-\Delta x)} \sum_{k=1}^{n(x-\Delta x)} \langle \Delta\tau_\kappa \rangle \quad (6)}$$

A) Let us assume that Va is the drift velocity of the ionizing particle and that each new produced electron gains ,per average, a time ρ2 relative to its father

$$\boxed{n(x)\langle T(x)\rangle - n(x)\langle T(x-\Delta x)\rangle = \sum_{k=1}^{n(x-\Delta x)} \langle \Delta t_k \rangle + \frac{\Delta n}{n(x-\Delta x)} \sum_{k=1}^{n(x-\Delta x)} \langle \Delta \tau_\kappa \rangle \quad (6)}$$

$$n(x)\langle T(x)\rangle - n(x)\langle T(x-\Delta x)\rangle = \sum_{k=1}^{n(x-\Delta x)} \langle \Delta t_k \rangle + \frac{\Delta n}{n(x-\Delta x)} \sum_{k=1}^{n(x-\Delta x)} \left[\langle \Delta t_\kappa \rangle - \rho_2\right] = \sum_{k=1}^{n(x-\Delta x)} \langle \Delta t_k \rangle + \frac{\Delta n}{n(x-\Delta x)} \sum_{k=1}^{n(x-\Delta x)} \langle \Delta t_\kappa \rangle - \frac{\Delta n}{n(x-\Delta x)} \sum_{k=1}^{n(x-\Delta x)} \rho_2$$

$$n(x)\langle T(x)\rangle - n(x)\langle T(x-\Delta x)\rangle = n(x-\Delta x)\langle \Delta t_k \rangle + \Delta n \langle \Delta t_k \rangle - \Delta n \rho_2 = n(x)\langle \Delta t_k \rangle - \Delta n \rho_2$$

$$\langle T(x)\rangle - \langle T(x-\Delta x)\rangle = \langle \Delta t_k \rangle - \frac{\Delta n}{n(x)}\rho_2 = \frac{\Delta x}{v_a} - \frac{\Delta n}{n(x)}\rho_2$$

for $\Delta x \to 0$

$$d\langle T(x)\rangle = \frac{dx}{v_a} - \rho_2 d\ln n(x) \quad or \quad \langle T(L)\rangle - \frac{L}{v_a} = -\rho_2 \ln n(L) + C \quad (7)$$

B) Let us assume that Vp is the drift velocity of the ionizing particle and that each new produced electron gains ,per average, a time ρ2 whilst the ionizing electron (just after the ionization) gains ρ1, relative to a non ionizing e of the avalanche

$$\boxed{n(x)\langle T(x)\rangle - n(x)\langle T(x-\Delta x)\rangle = \sum_{k=1}^{n(x-\Delta x)} \langle \Delta t_k \rangle + \frac{\Delta n}{n(x-\Delta x)} \sum_{k=1}^{n(x-\Delta x)} \langle \Delta \tau_\kappa \rangle \quad (6)}$$

$$n(x)\langle T(x)\rangle - n(x)\langle T(x-\Delta x)\rangle = \left(1 - \frac{\Delta n}{n(x-\Delta x)}\right) \sum_{k=1}^{n(x-\Delta x)} \langle \Delta t_k \rangle + \frac{\Delta n}{n(x-\Delta x)} \sum_{k=1}^{n(x-\Delta x)} \left[\langle \Delta t_\kappa \rangle - \rho_1\right] + \frac{\Delta n}{n(x-\Delta x)} \sum_{k=1}^{n(x-\Delta x)} \left[\langle \Delta t_\kappa \rangle - \rho_2\right]$$

$$= \sum_{k=1}^{n(x-\Delta x)} \langle \Delta t_k \rangle - \frac{\Delta n}{n(x-\Delta x)} \sum_{k=1}^{n(x-\Delta x)} \rho_1 + \frac{\Delta n}{n(x-\Delta x)} \sum_{k=1}^{n(x-\Delta x)} \langle \Delta t_\kappa \rangle - \frac{\Delta n}{n(x-\Delta x)} \sum_{k=1}^{n(x-\Delta x)} \rho_2$$

$$n(x)\langle T(x)\rangle - n(x)\langle T(x-\Delta x)\rangle = n(x-\Delta x)\langle \Delta t_k \rangle + \Delta n \langle \Delta t_k \rangle - \Delta n \rho_1 - \Delta n \rho_2 = n(x)\langle \Delta t_k \rangle - \Delta n(\rho_1 + \rho_2)$$

$$\langle T(x)\rangle - \langle T(x-\Delta x)\rangle = \langle \Delta t_k \rangle - \frac{\Delta n}{n(x)}(\rho_1 + \rho_2) = \frac{\Delta x}{v_p} - \frac{\Delta n}{n(x)}(\rho_1 + \rho_2)$$

for $\Delta x \to 0$

$$d\langle T(x)\rangle = \frac{dx}{v_p} - \overbrace{(\rho_1 + \rho_2)}^{\rho_{eff}} d\ln n(x) \quad (8) \quad or \quad \langle T(L)\rangle - \frac{L}{v_p} = -\rho_{eff} \ln n(L) + C \quad (9)$$

$$\bar{T}(L,n(L)) - \frac{L}{v} = -\rho \ln n(L) + c$$

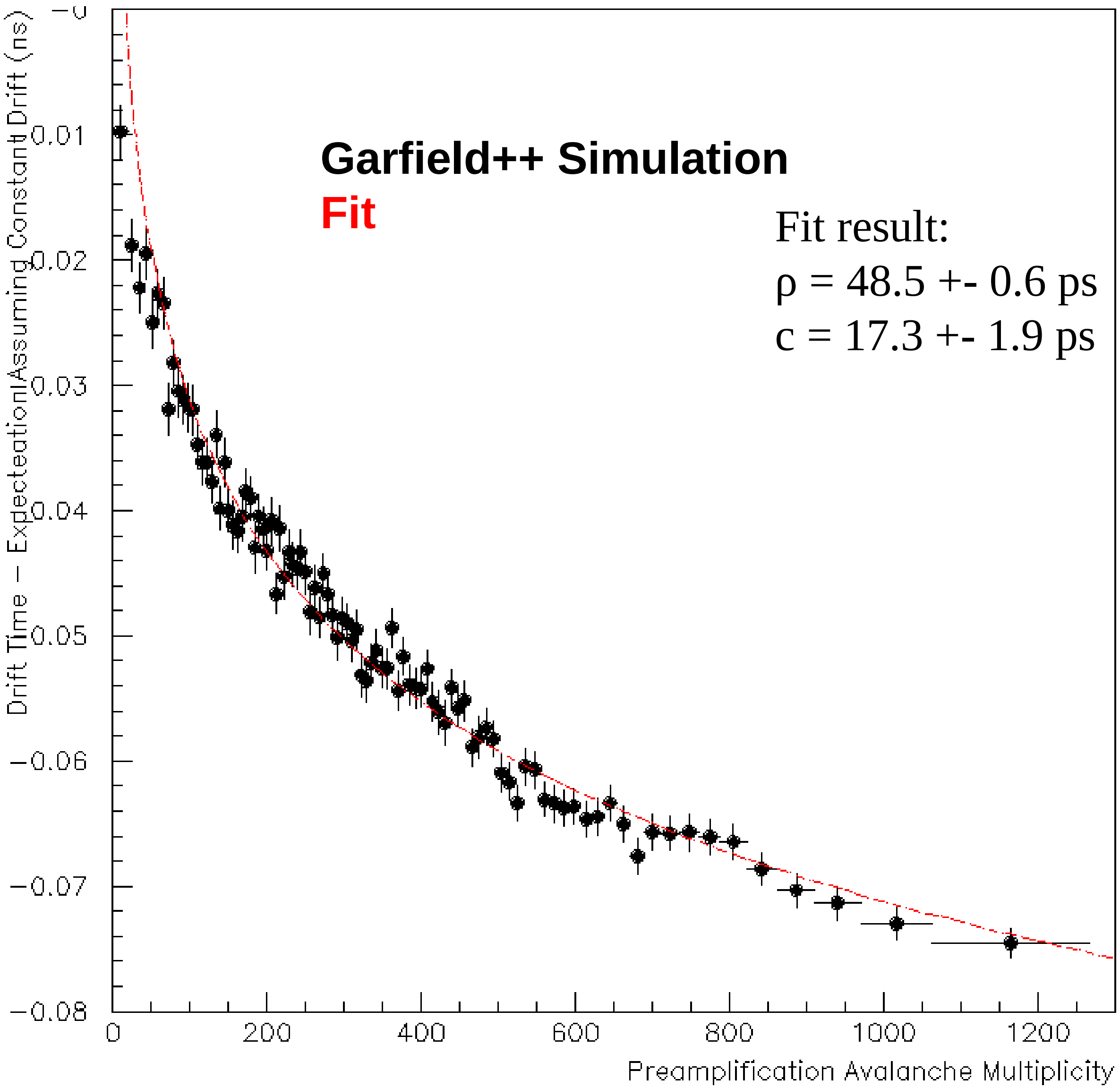

This model can perfectly describe the dependence of the avalanche's arrival time on the number of electrons.

By assuming the Polya (Gamma) distribution and integrating over all possible number of electrons…

$$\bar{T}_L = L\left[\frac{1}{v_a} - \rho_2 a_{eff}\right] + \left[-\rho_2 \ln 2 + C + \rho_2 \ln(\theta+1) - \rho_2 \psi(\theta+1)\right]$$

We predict again a linear dependence with a modified drift velocity in agreement with the Garfield++ simulation.

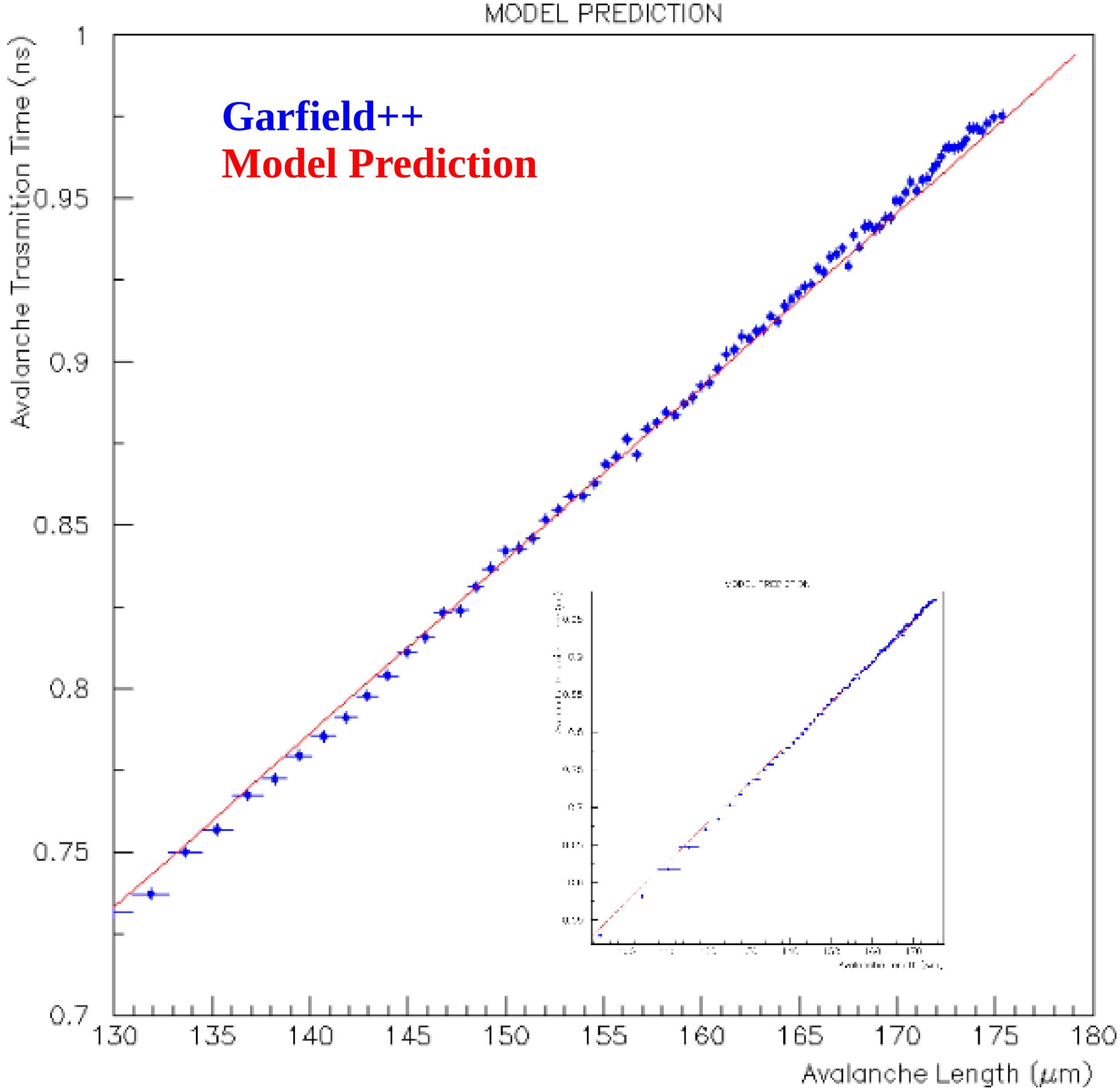

Integrating over all possible avalanche lengths...

The agreement between simulation and model are excellent.

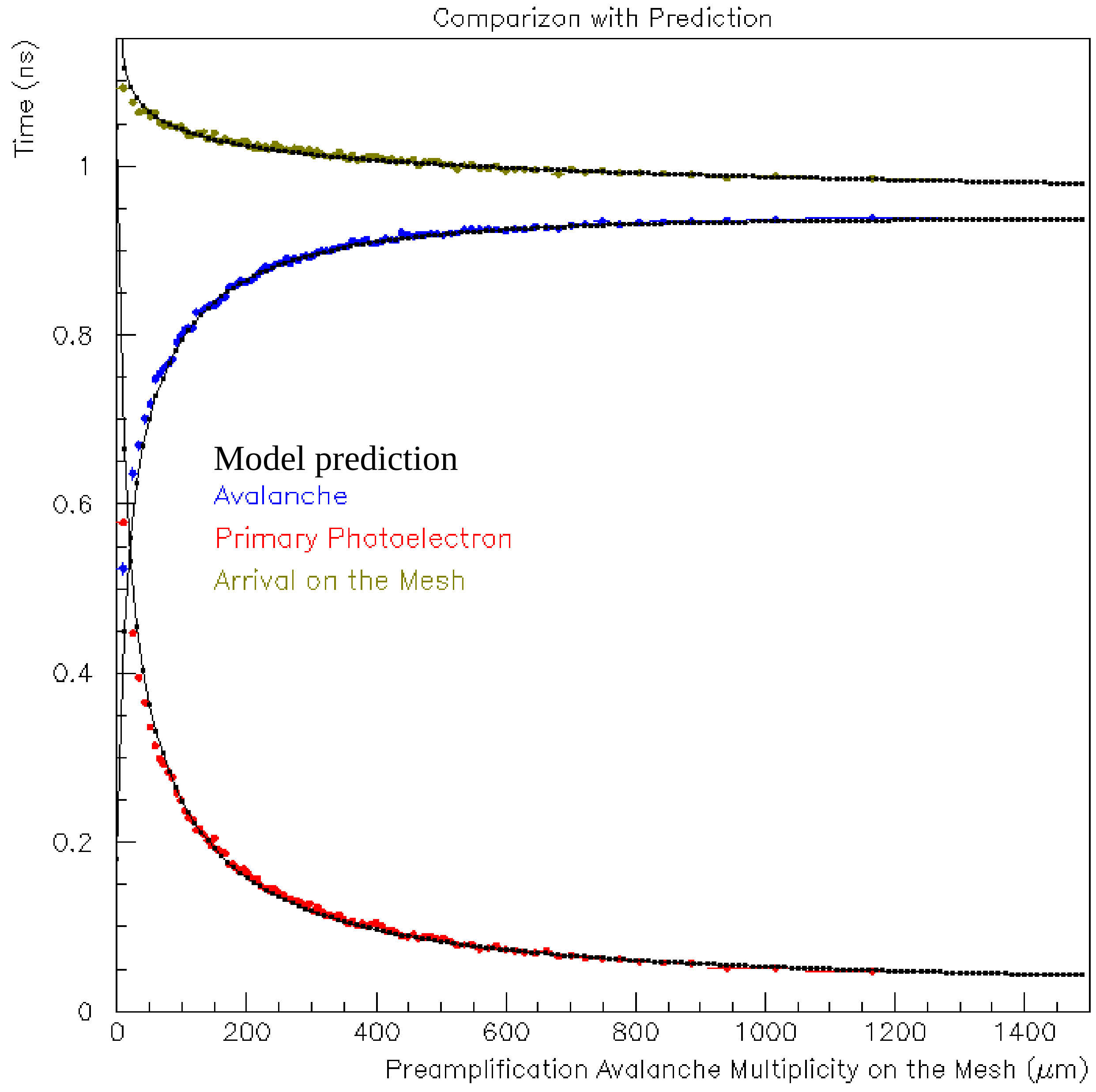

Proof 1: New electrons are created at x + Δx

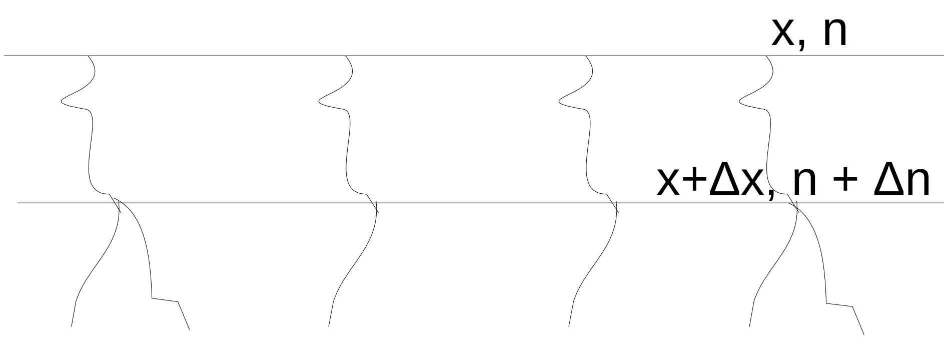

$$T_{n+\Delta n} = \frac{\sum_{i=1}^{n}(t_i+\tau_i) + \sum_{j=1}^{\Delta n}(t'_j+\tau'_j)}{n+\Delta n}$$

$$T_{n+\Delta n} = \frac{\sum_{i=1}^{n}(t_i+\tau_i) + \frac{\Delta n}{n}\sum_{i=1}^{n}(t_i+\tau_i)}{n+\Delta n}$$

$$T_{n+\Delta n} = \frac{(1+\frac{\Delta n}{n})\sum_{i=1}^{n}(t_i+\tau_i)}{n+\Delta n}$$

$$T_{n+\Delta n} = \frac{\sum_{i=1}^{n}(t_i+\tau_i)}{n}$$

$$V[T_{n+\Delta n}] = \frac{1}{n^2}\sum_{i=1}^{n}\sigma^2(t_i+\tau_i) + \sum_{i=1}^{n}\sum_{j=1, i\neq j}^{n}\frac{1}{n^2}\left(\langle(t_i+\tau_i)(t_j+\tau_j)\rangle - \langle(t_i+\tau_i)\rangle\langle(t_j+\tau_j)\rangle\right)$$

Old times are uncorrelated with new times:

$$V[T_{n+\Delta n}] = \frac{\sigma^2(x+\Delta x)}{n} + \frac{\mathrm{cov(x)}}{n^2}$$

$$V(x+\Delta x) - V(x) = \frac{\sigma^2(x+\Delta x)}{n} + \frac{\sigma^2(x)}{n}$$

$$dV(x) = \frac{d\sigma^2(x)}{n(x)}$$

Proof 2: New electrons are created at x

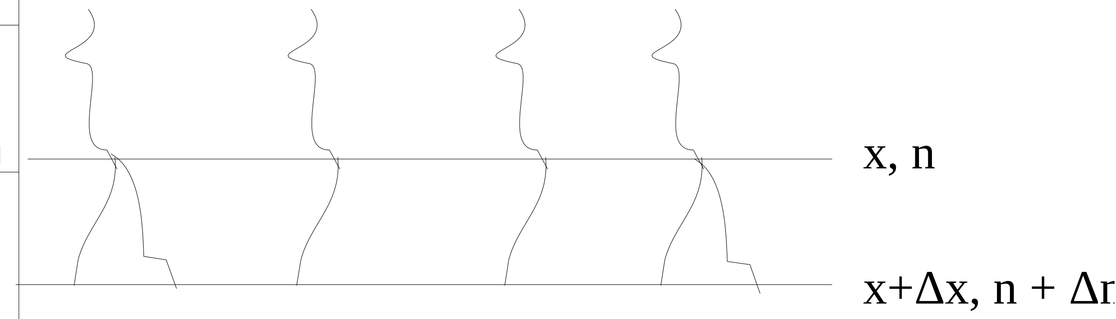

$$T(x+\Delta x) = \frac{\sum_{i=1}^{n} t_i}{n} + \frac{\sum_{i=1}^{n}\tau_i + \frac{\Delta n}{n}\sum_{i=1}^{n}\tau'_i}{n+\Delta n}$$

$$V(x+\Delta x) = \frac{\sigma^2(x)}{n} + \frac{\mathrm{cov}(x)}{n^2} + \frac{n\Delta\sigma^2(x) + \left(\frac{\Delta n}{n}\right)^2 n\Delta\sigma^2(x)}{(n+\Delta n)^2}$$

$$V(x+\Delta x) - V(x) = \frac{n\Delta\sigma^2(x) + \left(\frac{\Delta n}{n}\right)^2 n\Delta\sigma^2(x)}{(n+\Delta n)^2}$$

$$V(x+\Delta x) - V(x) = \frac{n^2 + (\Delta n)^2}{n(n+\Delta n)^2}\Delta\sigma^2(x)$$

$$\Delta x) - V(x) = \frac{(n+\Delta n)^2 - 2n\Delta n}{n(n+\Delta n)^2}\Delta\sigma^2(x)$$

$$V(x+\Delta x) - V(x) = \frac{\Delta\sigma^2(x)}{n} - \frac{2\Delta n}{(n+\Delta n)^2}\Delta\sigma^2(x)$$

$$dV(x) = \frac{d\sigma^2(x)}{n} - \frac{2dn}{(n+dn)^2}d\sigma^2(x)$$

$$V(L|n(x)) = \frac{2D_L}{v_d^3} \int_0^L \frac{1}{n(x)} dx$$

By averaging over all possible number of electrons...

The time spread of the avalanche's arrival time is predicted.

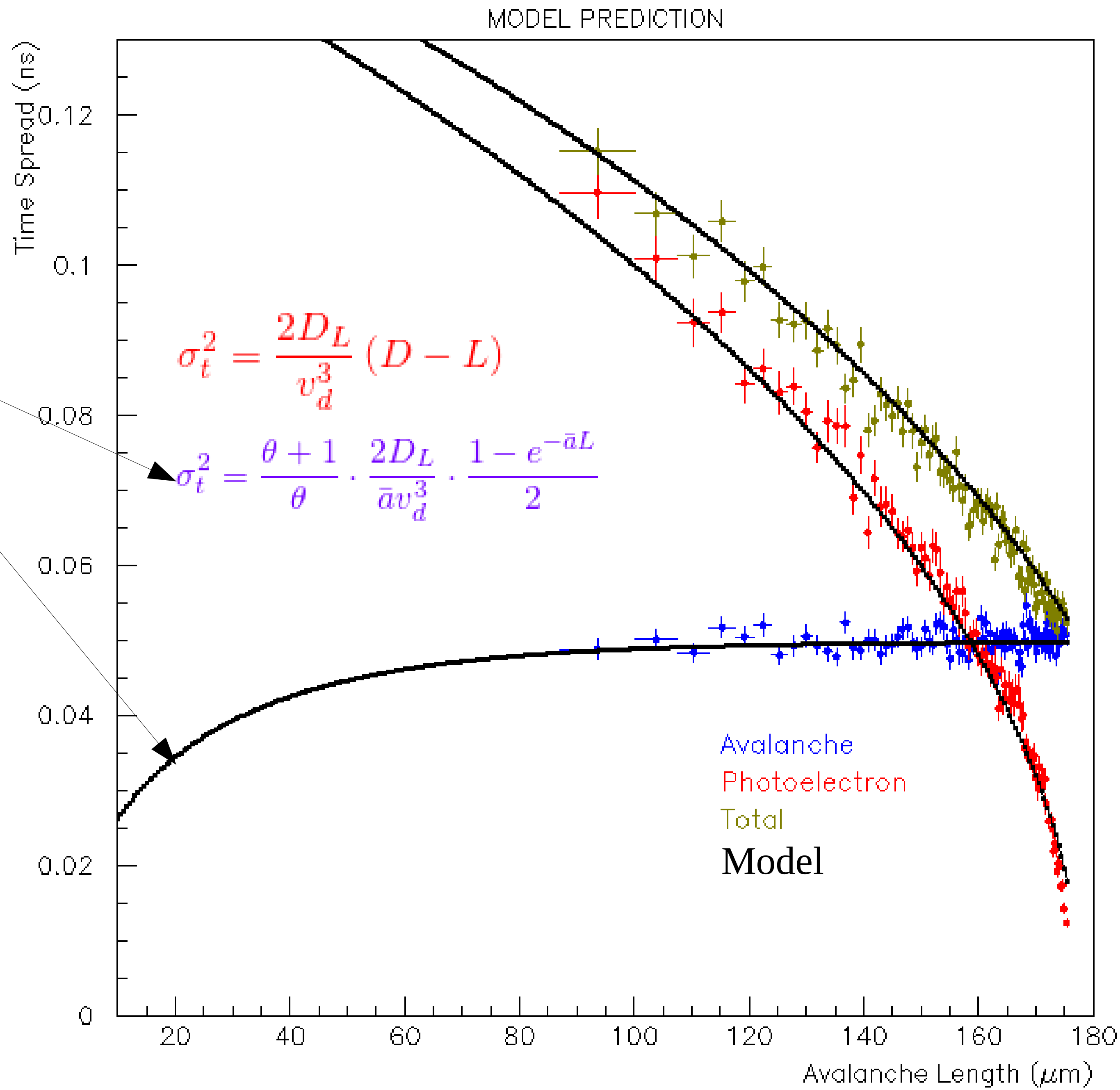

Exponential Growth

$$V(L|n(x)) = \frac{2D_L}{v_d^3}\int_0^L \frac{1}{n(x)}dx$$

If we want to express the variance in terms of the number of electrons, we need the mean number of electrons as a function of the distance from the avalanche creation, **given that in the end N electrons were produced.**

The initial multiplication is decisive for the final size of the avalanche. Once it has reached a size of 100-1000 electrons, it will continue exponentially.

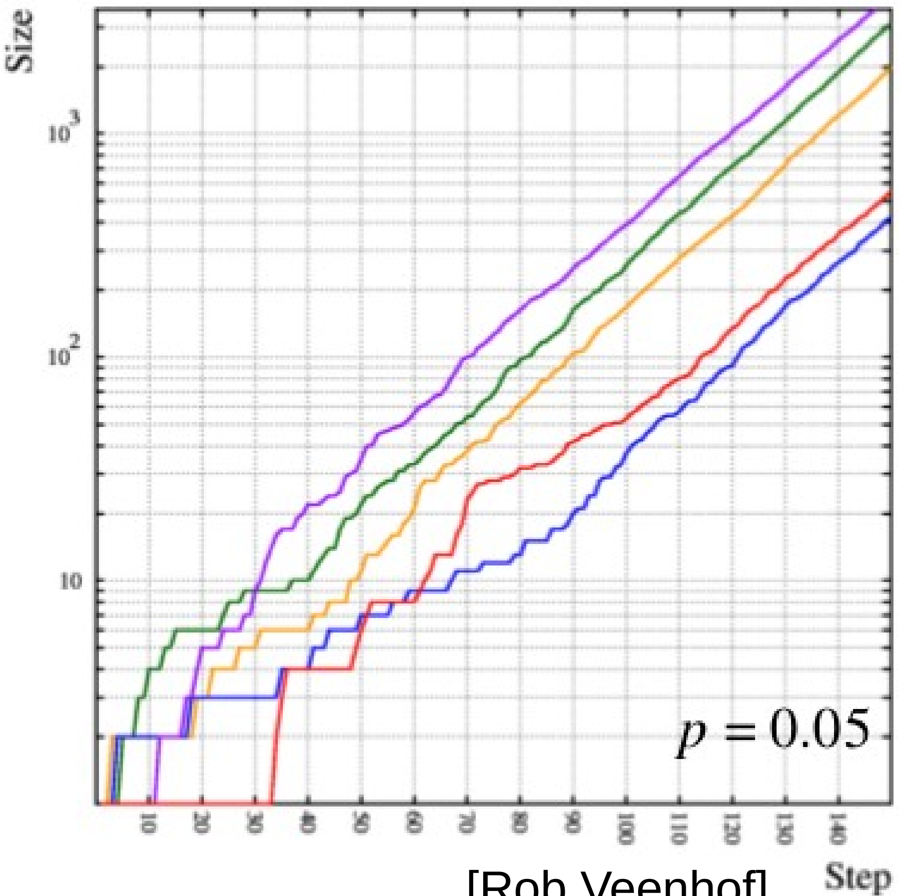

[Rob Veenhof]

Exponential Growth

$$q(L - \Delta x|N_L) = N_L - q(L - \Delta x|N_L) \cdot a \cdot \Delta x$$

$$q(L - \Delta x|N_L) = \frac{N_L}{1 + a\Delta x}$$

$$q(L - 2\Delta x|N_L) = \frac{N_L}{(1 + a\Delta x)^2}$$

$$q(L - n\Delta x|N_L) = \frac{N_L}{(1 + a\Delta x)^n}$$

$$q(L - x|N_L) = \lim_{n\to\infty} \frac{N_L}{\left(1 + \frac{ax}{n}\right)^n}$$

$$q(y|N_L) = \frac{N_L}{\langle N_L \rangle} N_0 e^{ay}$$

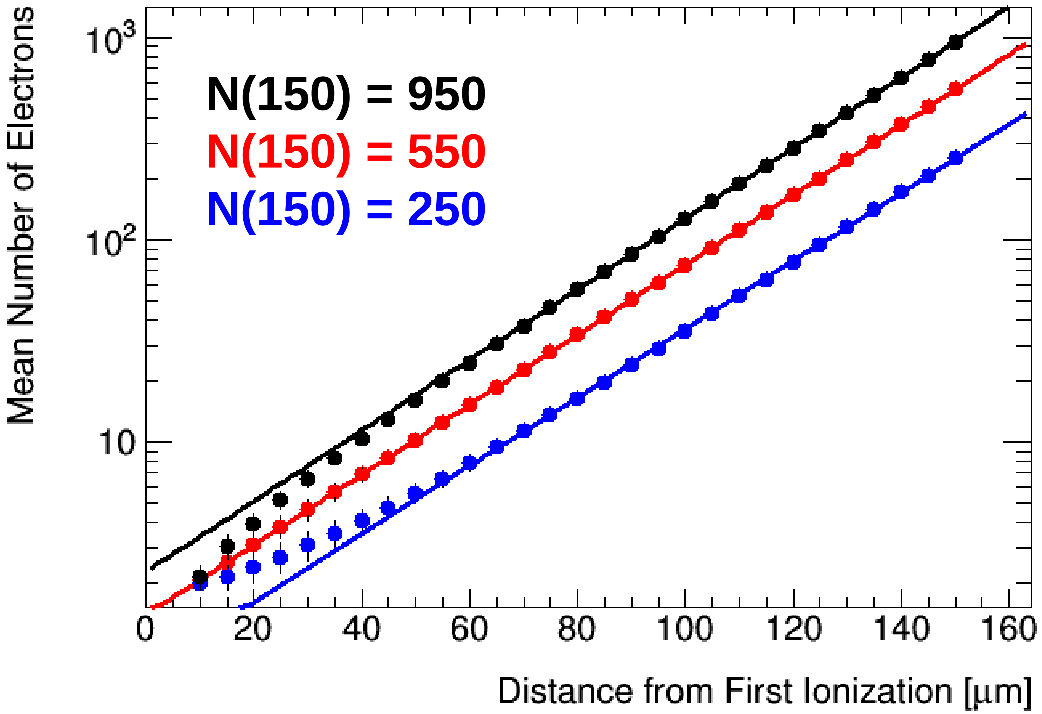

$$V(N_L|L) = \frac{2D_L}{\bar{a}v_d^3}\frac{\langle N_L\rangle - N_0}{N_L N_0}$$

By integrating over all possible lengths of avalanches...

$$V(n) = \int_{x_1}^{x_2} V(n|L)G(L|n)dL$$
$$+ \int_{x_1}^{x_2} \left(\langle T(L,n)\rangle\right)^2 G(L|n)dL$$
$$- \left(\int_{x_1}^{x_2} \langle T(L,n)\rangle G(L|n)dL\right)^2$$

Spread caused by “slewing” of the mean time on length of avalanche.

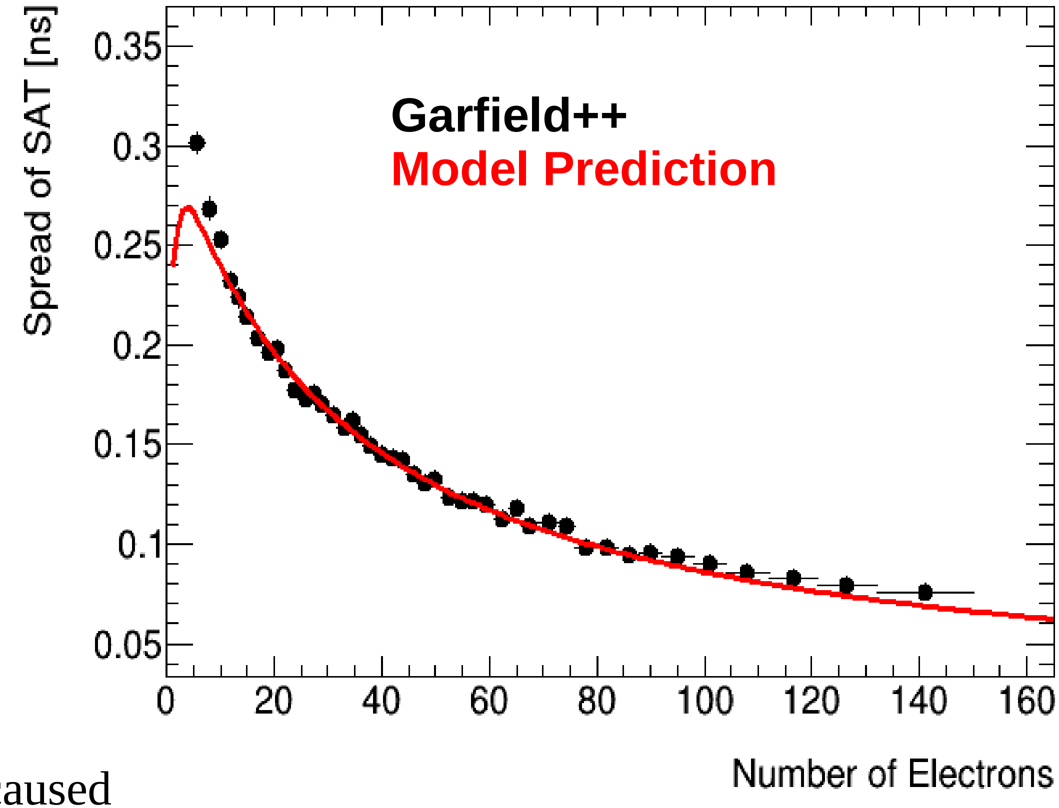

Conclusions

- We report an excellent time resolution below 80 ps for single photoelectrons using both the COMPASS and the CF4-based mixtures.
- We observe some interesting timing characteristics and developed a simulation tool based on Garfield++ to also take into account the electronics in a data driven way.
- We pinpointed to the mechanism that produces the observed time walk, i.e. that larger signals arrive faster than smaller ones.
- We developed a phenomenological model to help us understand the rest of the observed effects and we are ready to see how the parameters of the model behave by changing the Drift Voltage.
- It should be emphasized that we do not intend to replace Garfield++. We simply want to understand and pinpoint the physical processes that produce the timing characteristics. Garfield++ is still needed for the estimation of the model's parameters.

I thank you for your attention!

Backup Slides

Analysis of Simulation

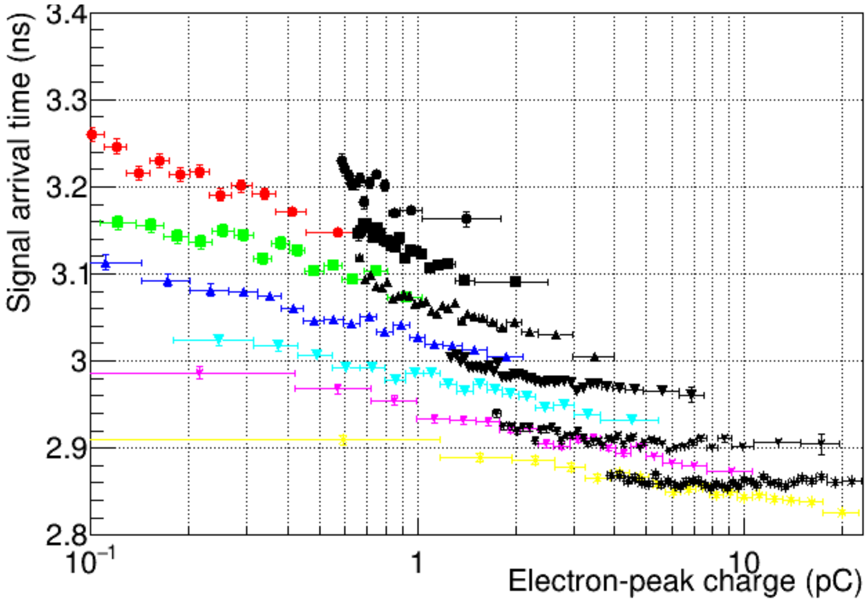

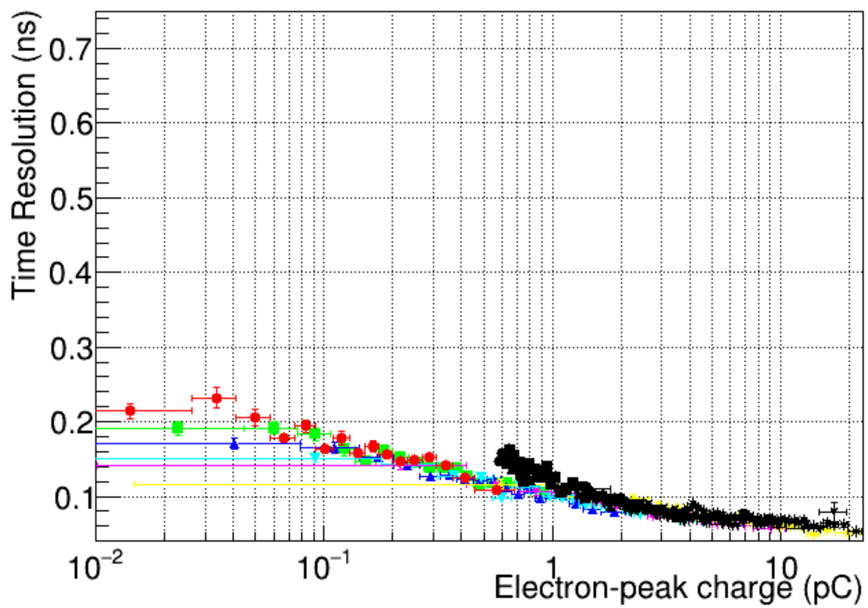

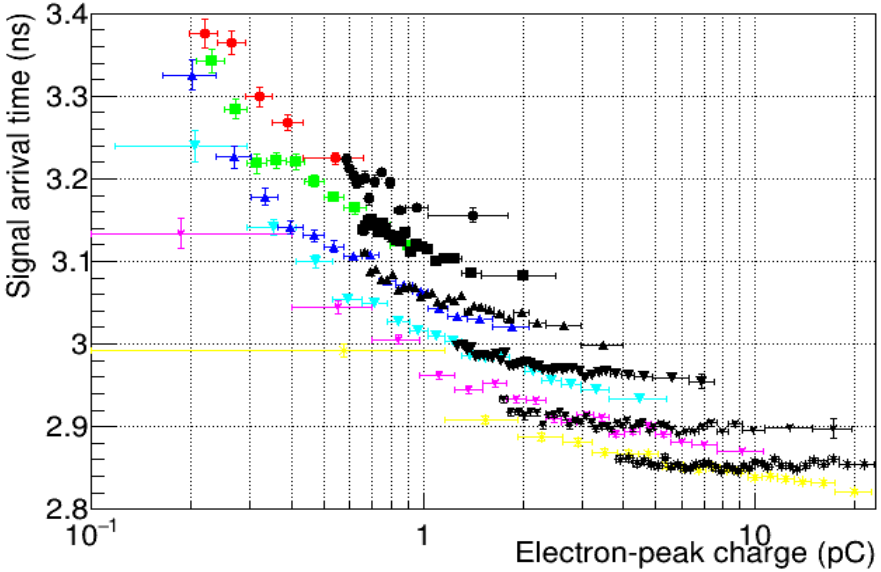

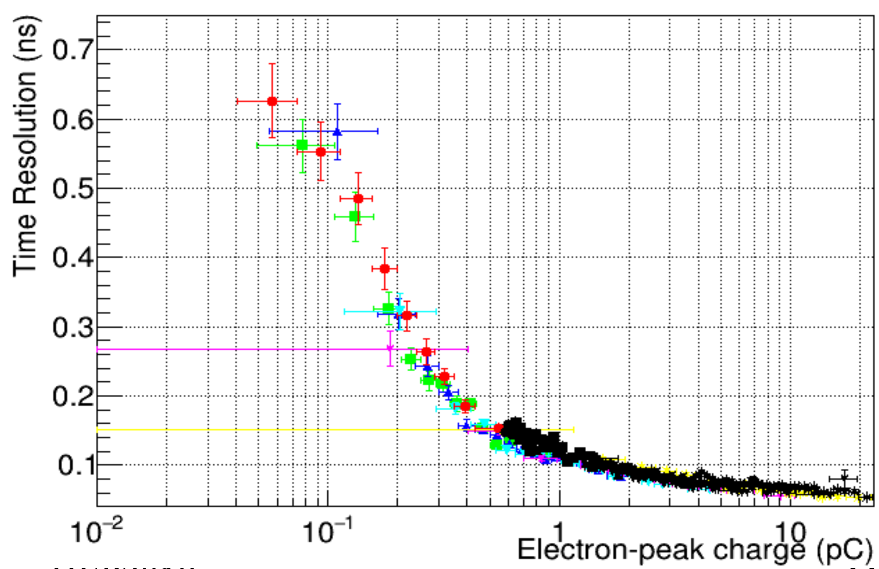

Single Electron Tracking

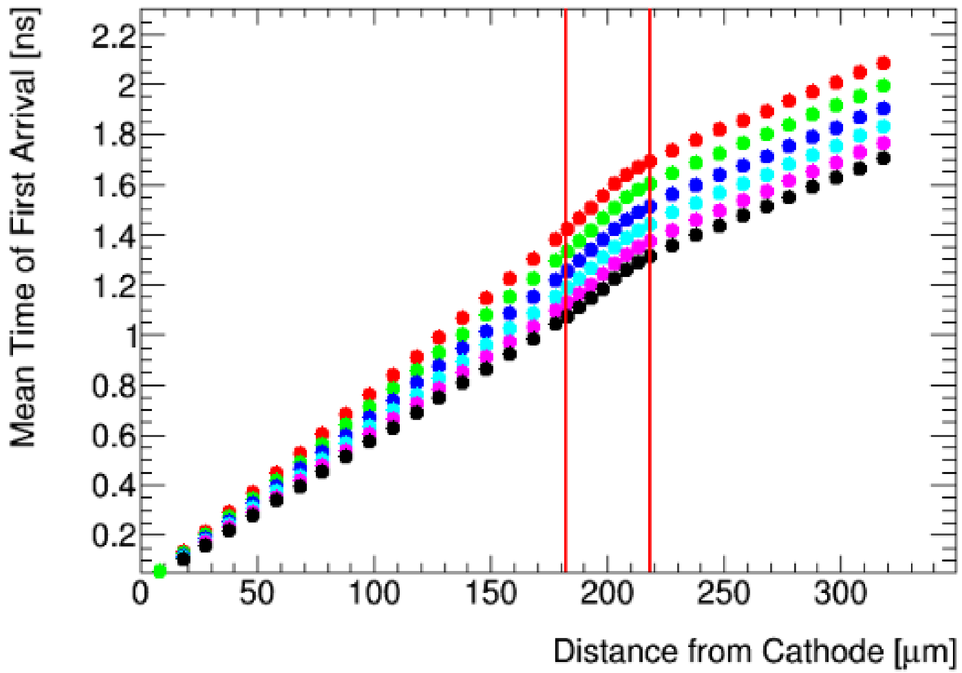

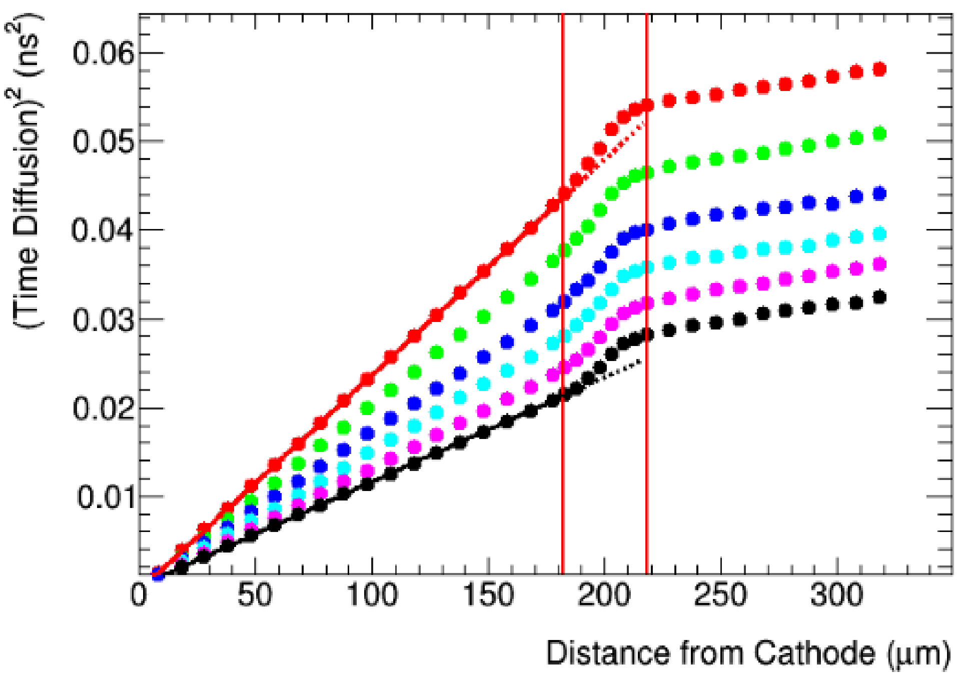

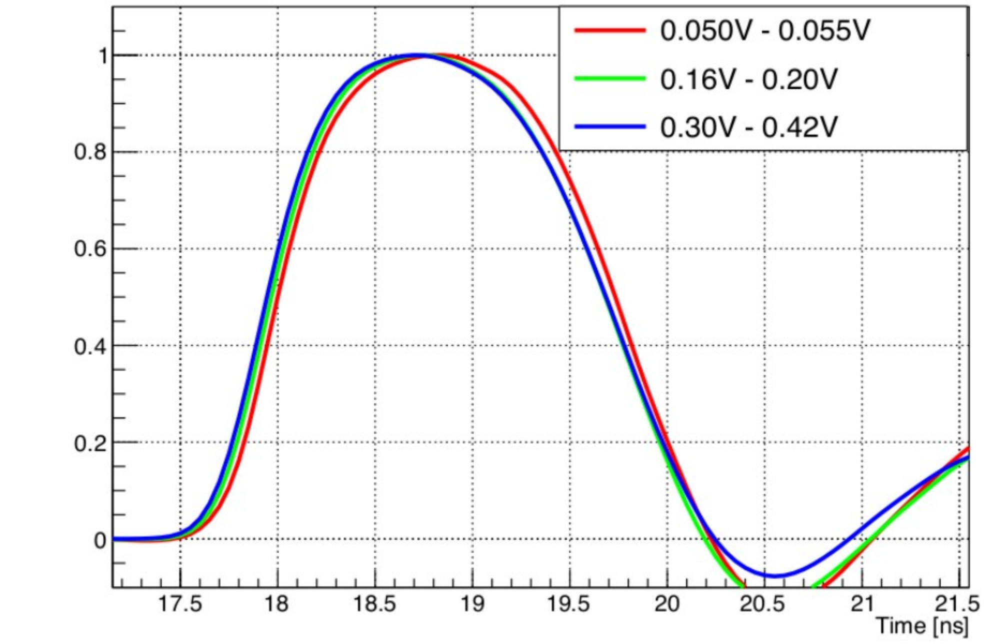

0.050V - 0.055V
0.16V - 0.20V
0.30V - 0.42V
Time [ns]

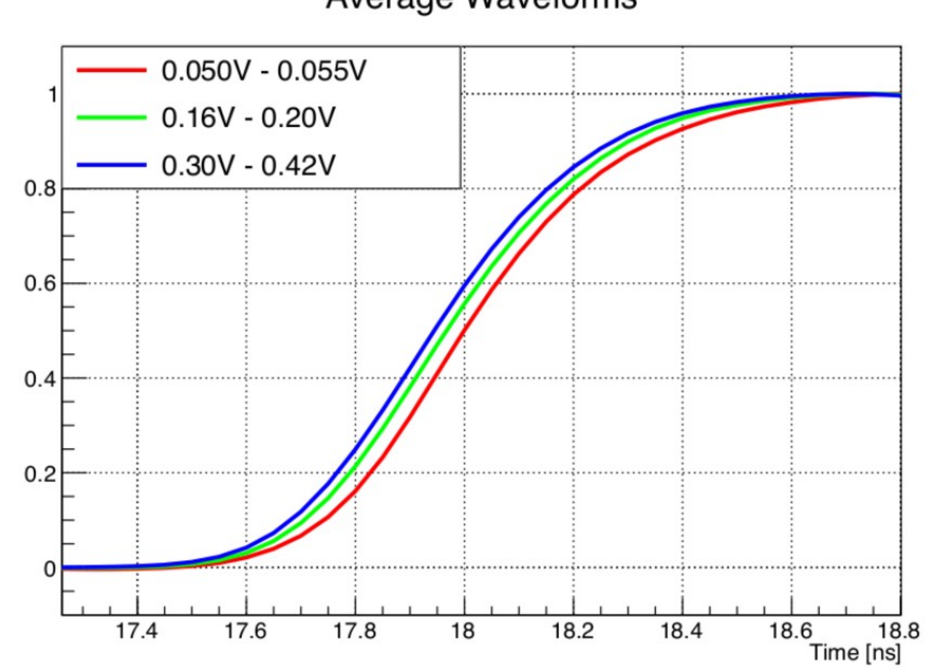

0.050V - 0.055V
0.16V - 0.20V
0.30V - 0.42V
Time [ns]

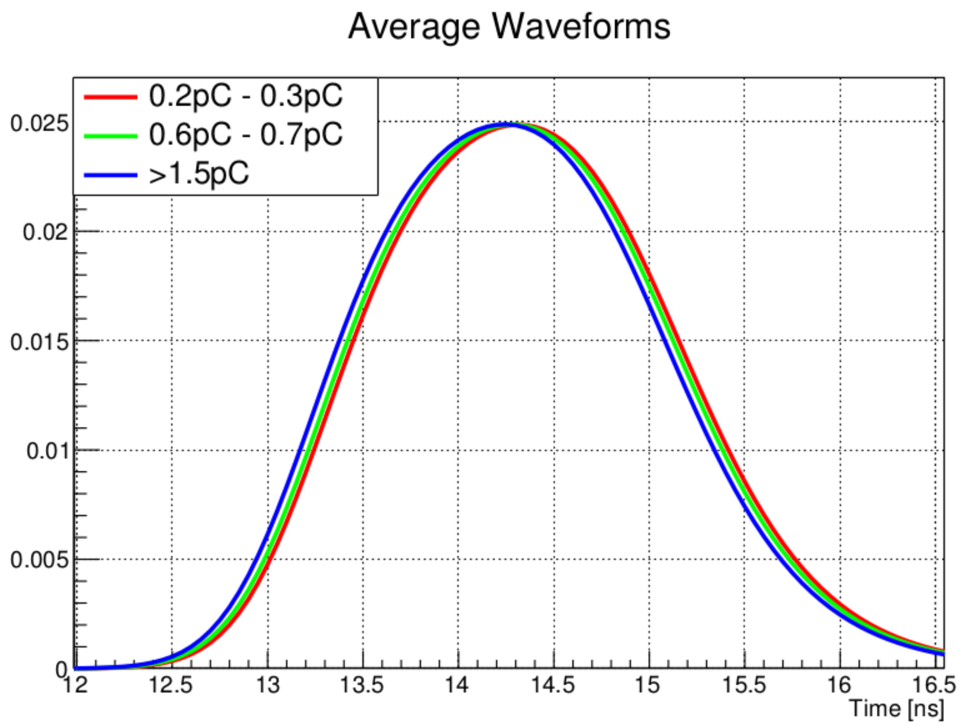

Average Waveforms
0.2pC - 0.3pC
0.6pC - 0.7pC
>1.5pC
Time [ns]

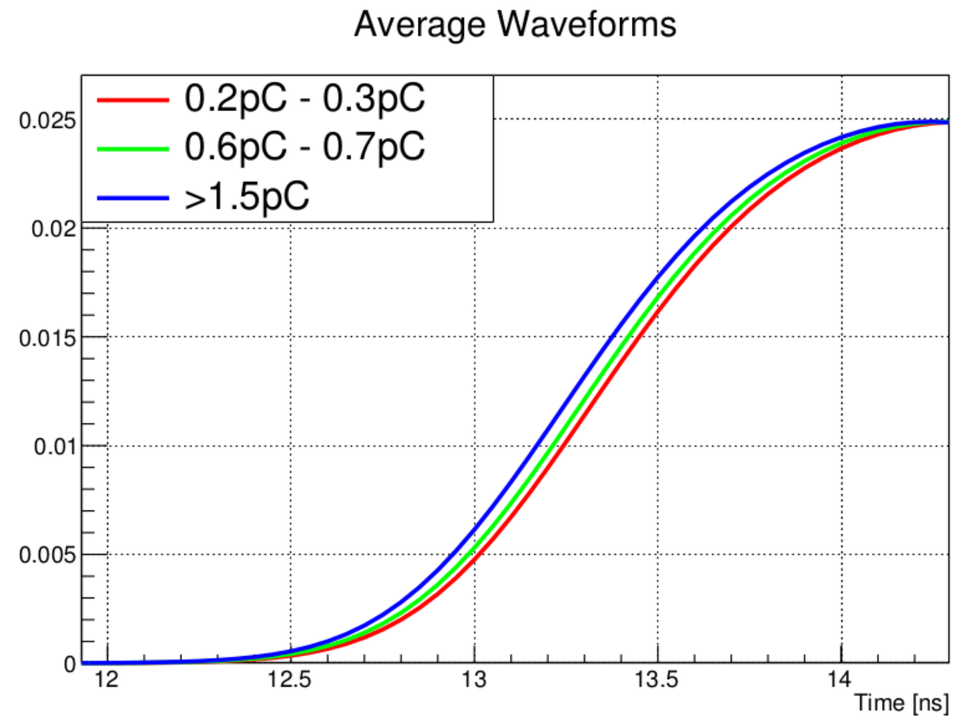

Average Waveforms
0.2pC - 0.3pC
0.6pC - 0.7pC
>1.5pC
Time [ns]

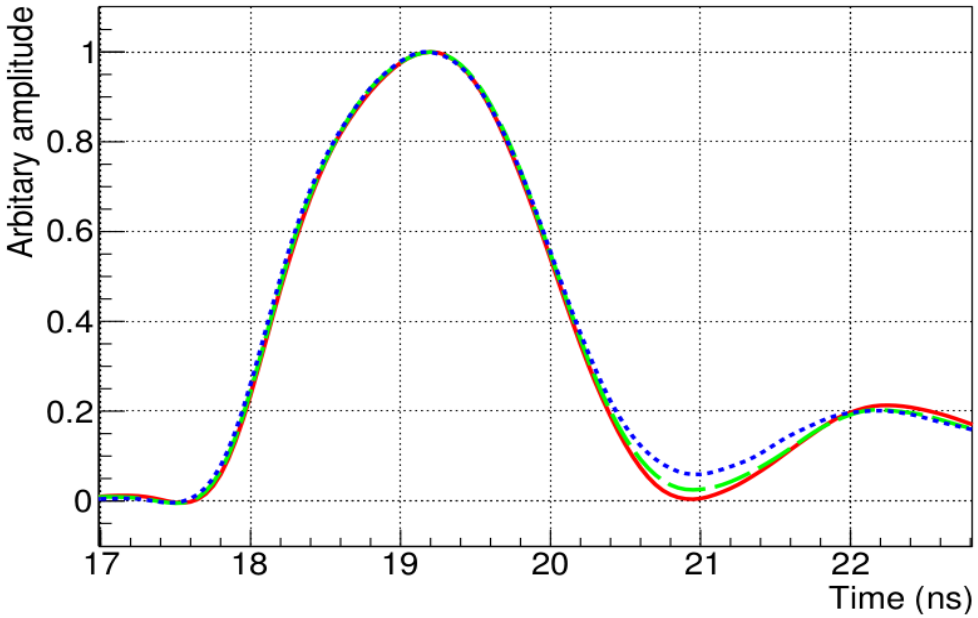
Arbitary amplitude
Time (ns)

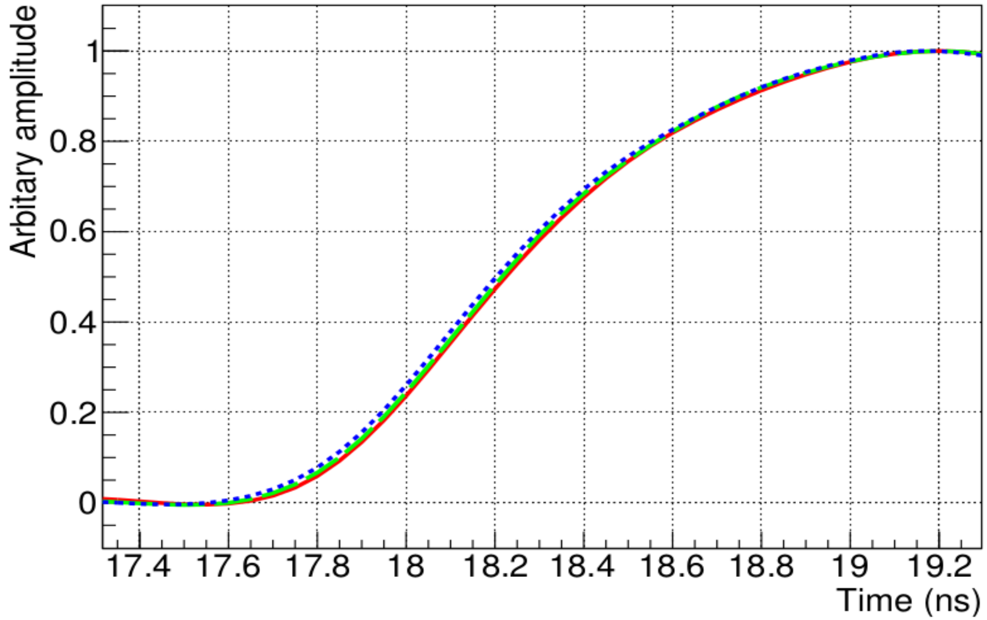
Arbitary amplitude
Time (ns)

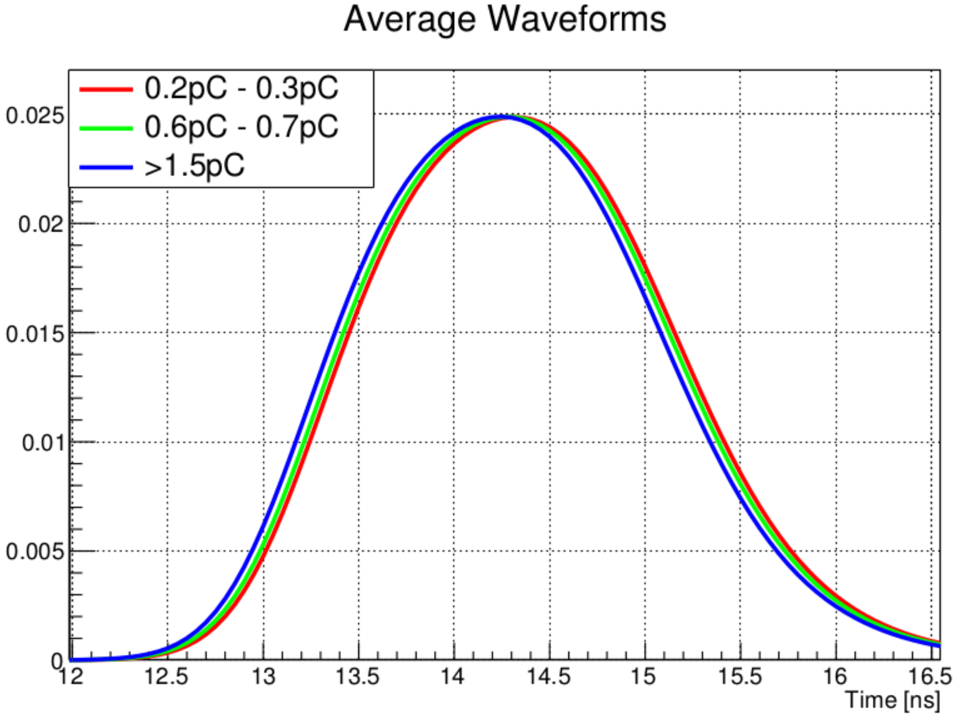
Average Waveforms
0.2pC - 0.3pC
0.6pC - 0.7pC
>1.5pC
Time [ns]

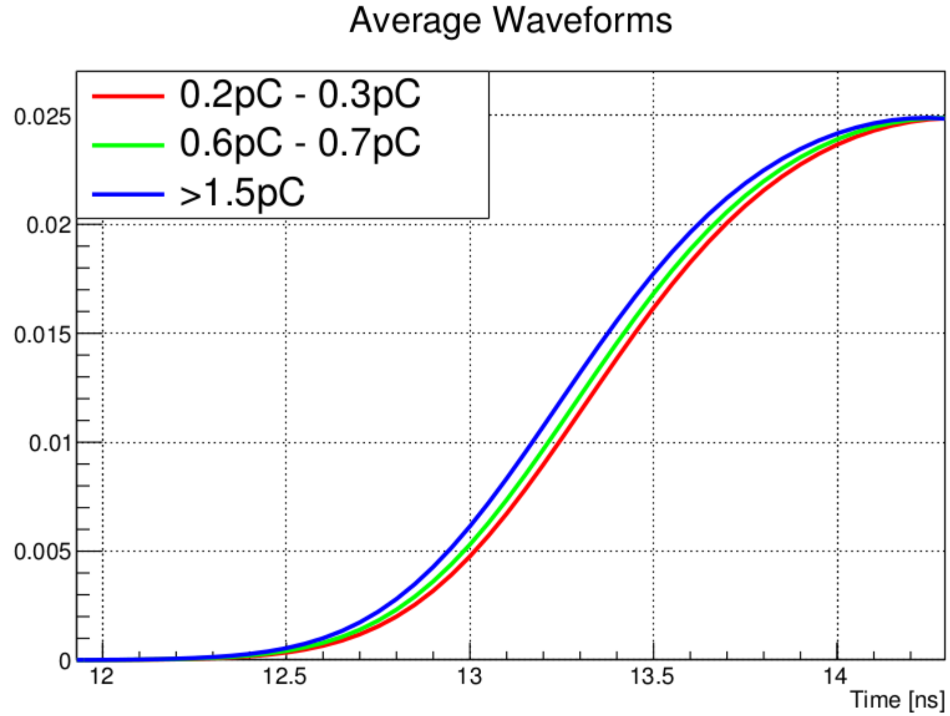
Average Waveforms
0.2pC - 0.3pC
0.6pC - 0.7pC
>1.5pC
Time [ns]

Drift Voltage = 350 V

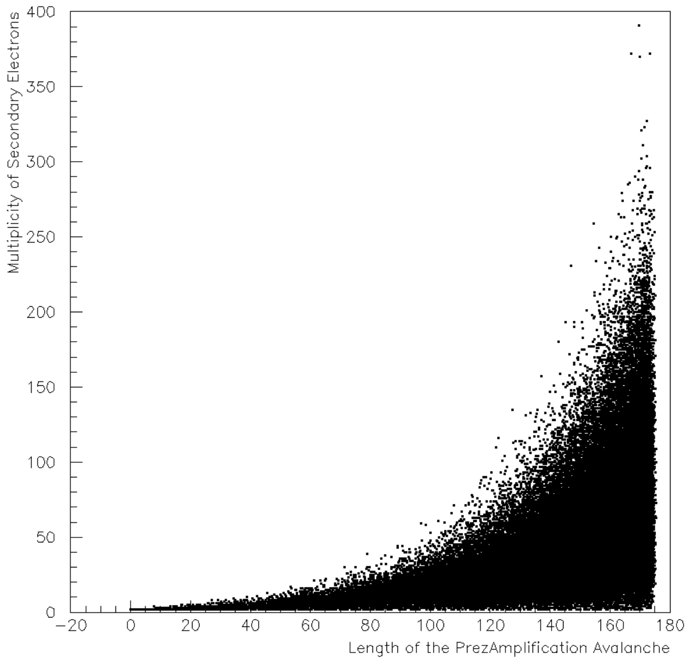

Fig: Scatter plot of secondary electron multiplicity vs pre-amplification avalanche length.

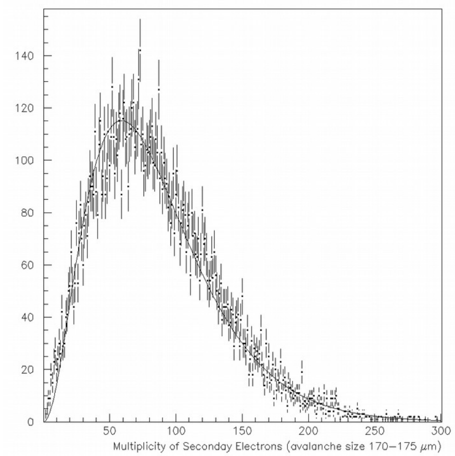

Fig: Distribution of secondary electrons' multiplicity for pre-amplification avalanche length in [170μm - 175μm]

In a small region of pre-amplification avalanche lengths, we parameterize the distribution of the number of secondary electrons with the Polya distribution.

We fit Polya distributions in all bins and find that both the **Mean** and the **RMS** values follow exponential laws with the same rate parameters.

This means that the shape parameter of the Polya remains constant across the multiplication process.

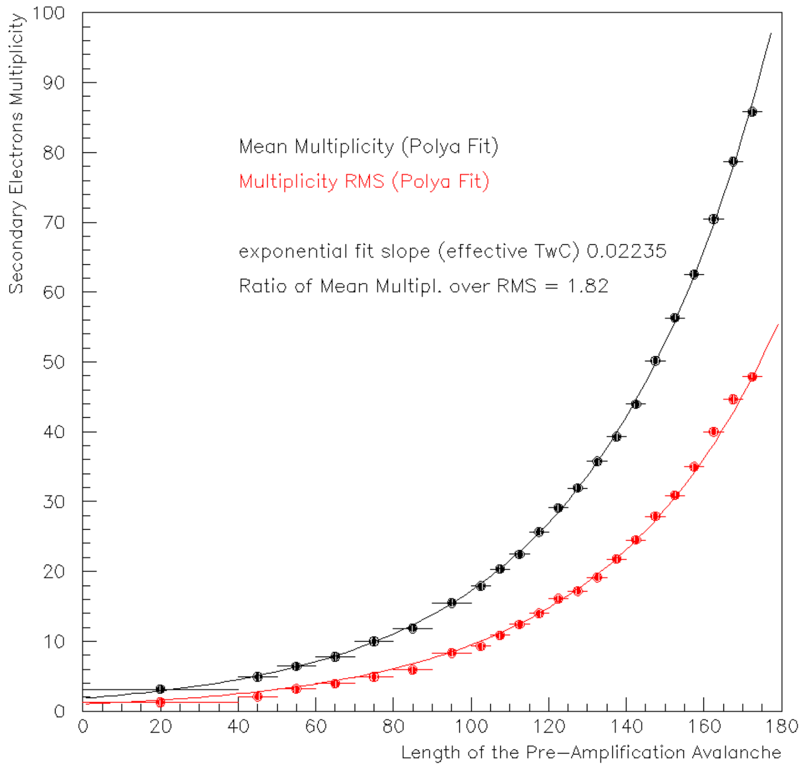

Fig: **Mean** and **RMS** values of Polya fits.

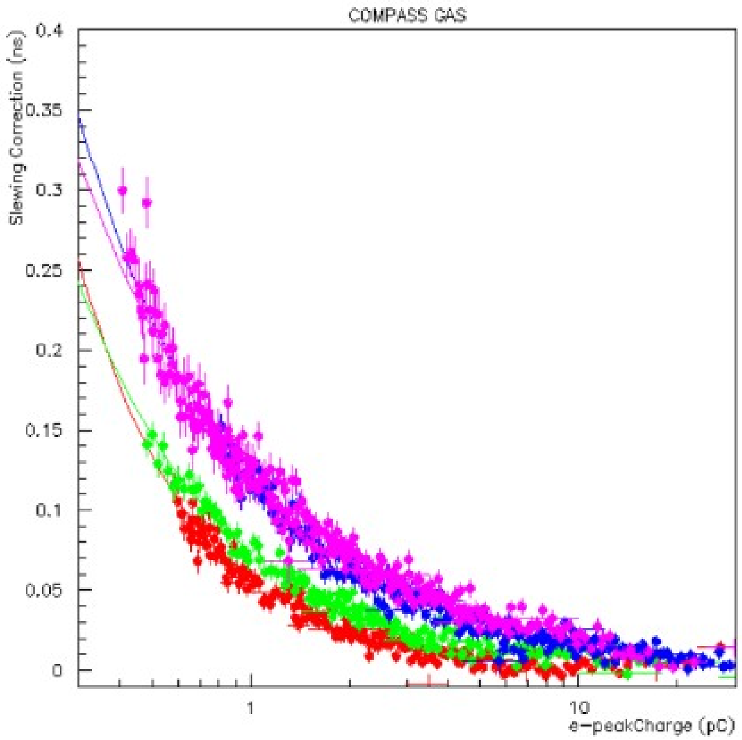

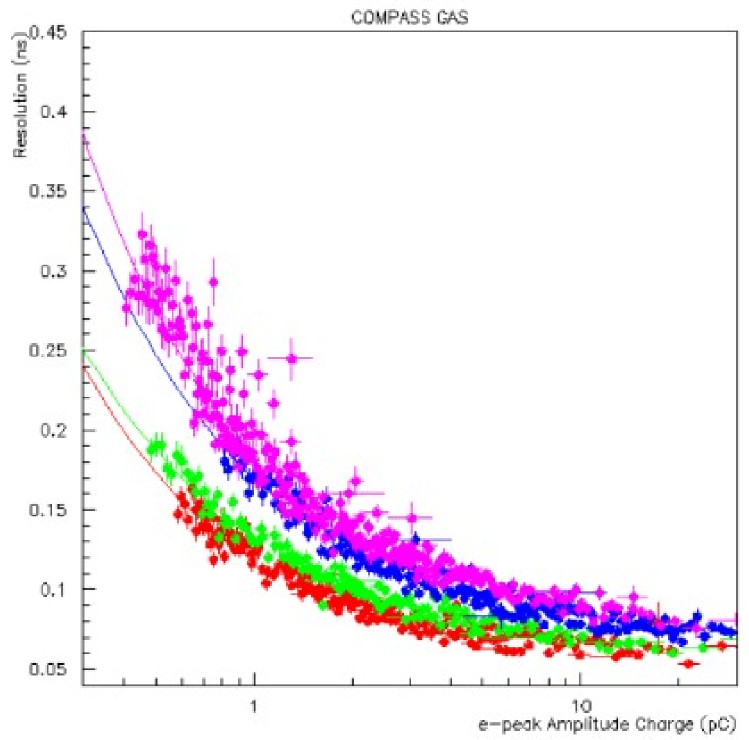

$$\sum_{i=1}^{N} a_i^2 \cdot V_i + \sum_{i=1}^{N} a_i a_j \left(V_i + V_j + (\mu_i - \mu_j)^2 \right)$$

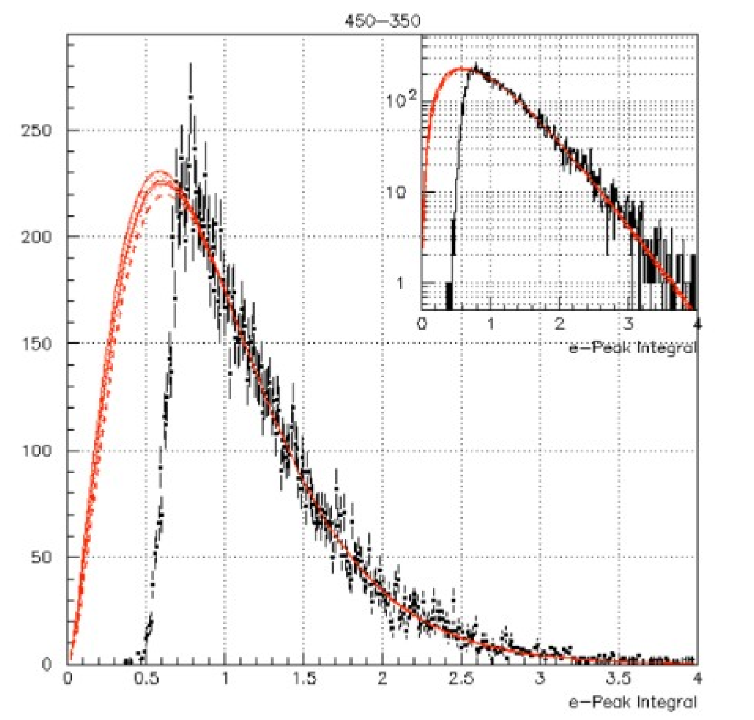

Inverse Gaussian as Time of Arrival Distribution at Constant Drift and Diffusion.

Consider a moving Gaussian(x) expressing difusion under drift Voltage with ·

$$\langle x \rangle = \mu = v_{drift} \cdot t$$

$$\langle (x-\mu)^2 \rangle = \sigma^2 = 2D_L \cdot t$$

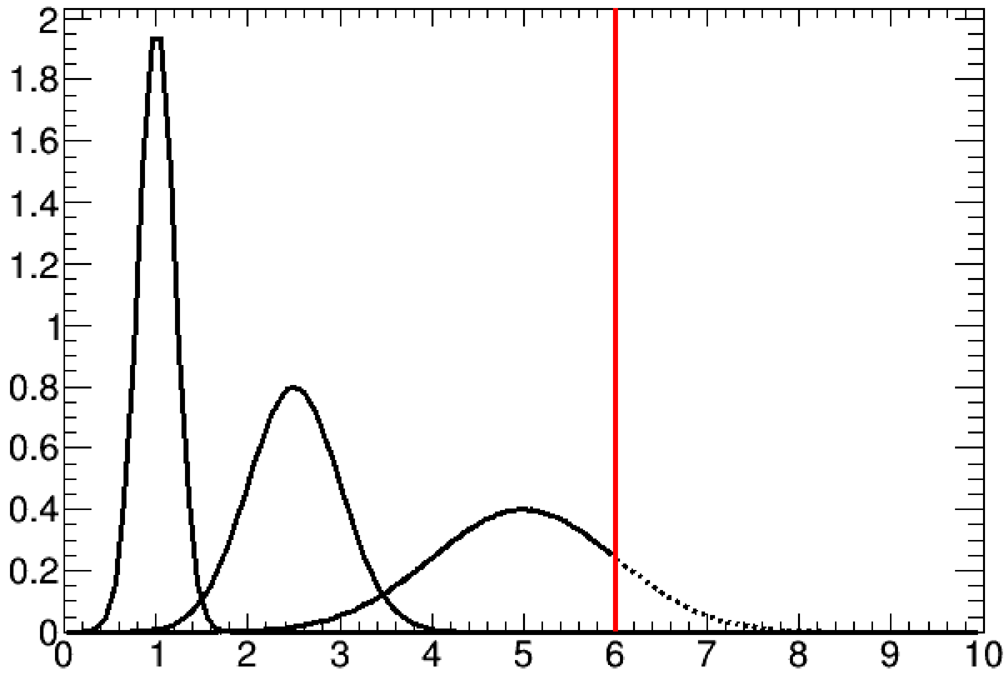

$$G(x;t) = \frac{1}{\sqrt{2\pi\sigma^2(t)}} e^{-\frac{(x-\mu(t))^2}{2\sigma^2(t)}}$$

$$C(t) = \int_a^\infty G(x;t)dx$$

Integrate the Gaussian from a fixed level “a” until Infinity.

This CDF is also CDF of the Time of Arrival at “a” .

$$P(t) = \frac{dC(t)}{dt} = \frac{-1}{\sqrt{\pi}} \frac{d}{dt} \left(\int_\infty^{\left(\frac{a-\mu(t)}{\sqrt{2}\sigma(t)}\right)} e^{-u^2} du \right)$$

Take derivative w.r.t. time to transform the CDF to PDF.

$$\boxed{P(t) = \sqrt{\frac{a^2}{2D_L}} \cdot \sqrt{\frac{1}{2\pi t^3}} \exp\left(-\frac{1}{2} \cdot \frac{a^2}{2D_L} \cdot \frac{v_d^2}{a^2} \cdot \frac{1}{t} \cdot \left(\frac{a}{v_d} - t \right)^2 \right)}$$

The resulted PDF is Inverse-Gaussian with mean $\mu = \frac{a}{v_d}$ and a shape parameter $\lambda = \frac{a^2}{2D_L}$